

Quantum Dots

2014. 5. 8.

Changhee Lee

School of Electrical Engineering and Computer Science
Seoul National Univ.
chlee7@snu.ac.kr



Part I: Properties and formation of semiconductor Quantum dots

- : Introduction*
- : Basic quantum mechanics applied to quantum dots (QDs)*
- : Basic properties of quantum wells and dots*
- : Formation of quantum dots*

Part II: Colloidal Quantum dot LEDs

- : QD-LED device structures and operating mechanism*
- : QD-LED device performance: Red, Green and Blue*
- : Exciton recombination and energy transfer*
- : Inverted QD-LEDs*
- : Polymer-QD hybrid LEDs*

Part III. QD and Hybrid Solar Cells



Part I: Properties and formation of semiconductor Quantum dots

: Introduction

: Basic quantum mechanics applied to quantum dots (QDs)

: Basic properties of quantum wells and dots

: Formation of quantum dots

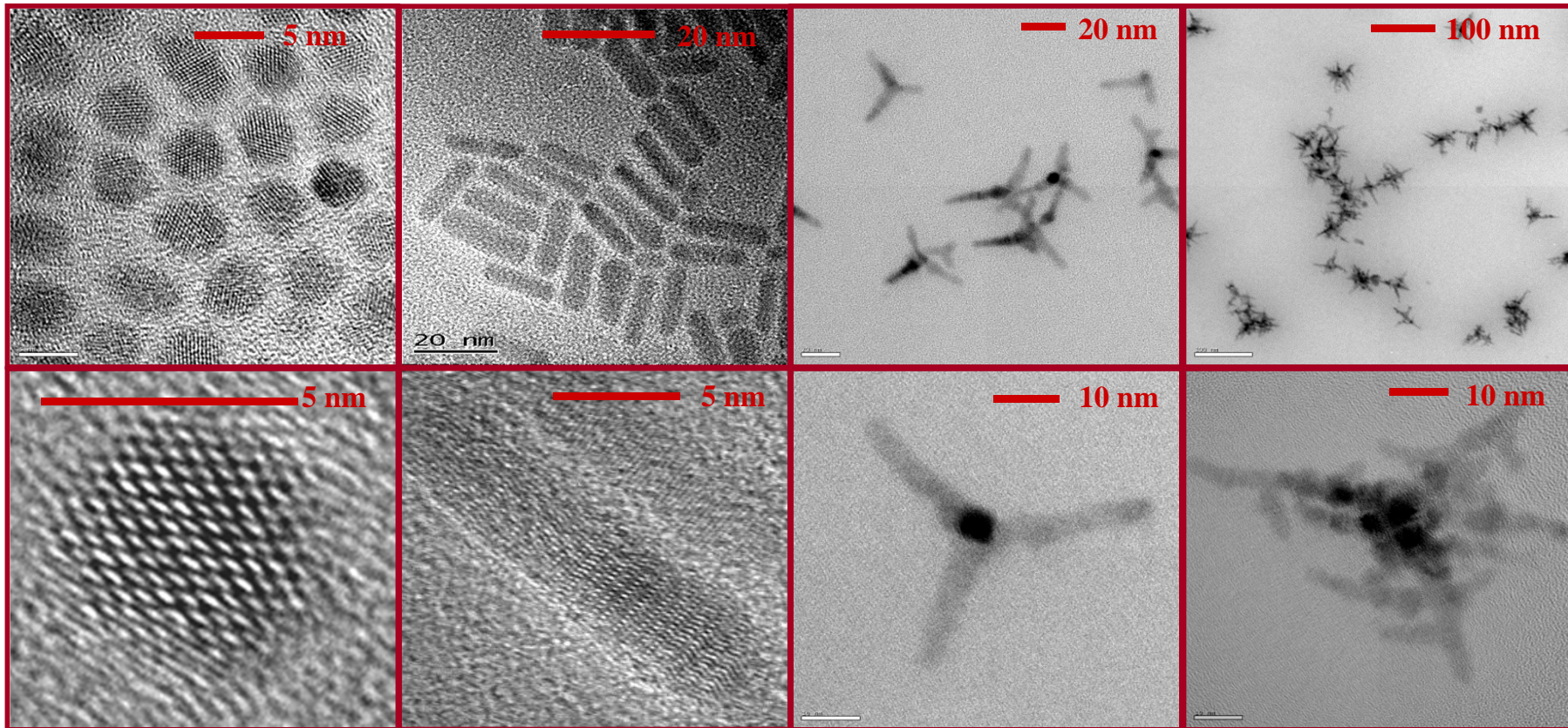


Dot

Rod

Tetrapod

Hyper-branched



synthesized by S. H. Lee's Group (SNU)

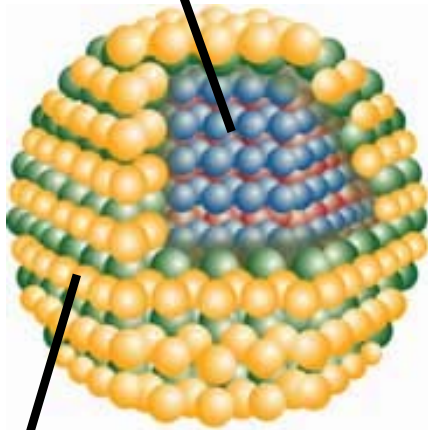
Quantum dots (QDs)

- Quantum dots?

“fragments of semiconductor consisting of hundreds to many thousands of atoms - with the bulk bonding geometry and with surface states eliminated by enclosure in a material that has a larger band gap” (A. P. Alivisatos, Science **271**, 933 (1996).)

→ excitons are confined in all three dimensions of space.

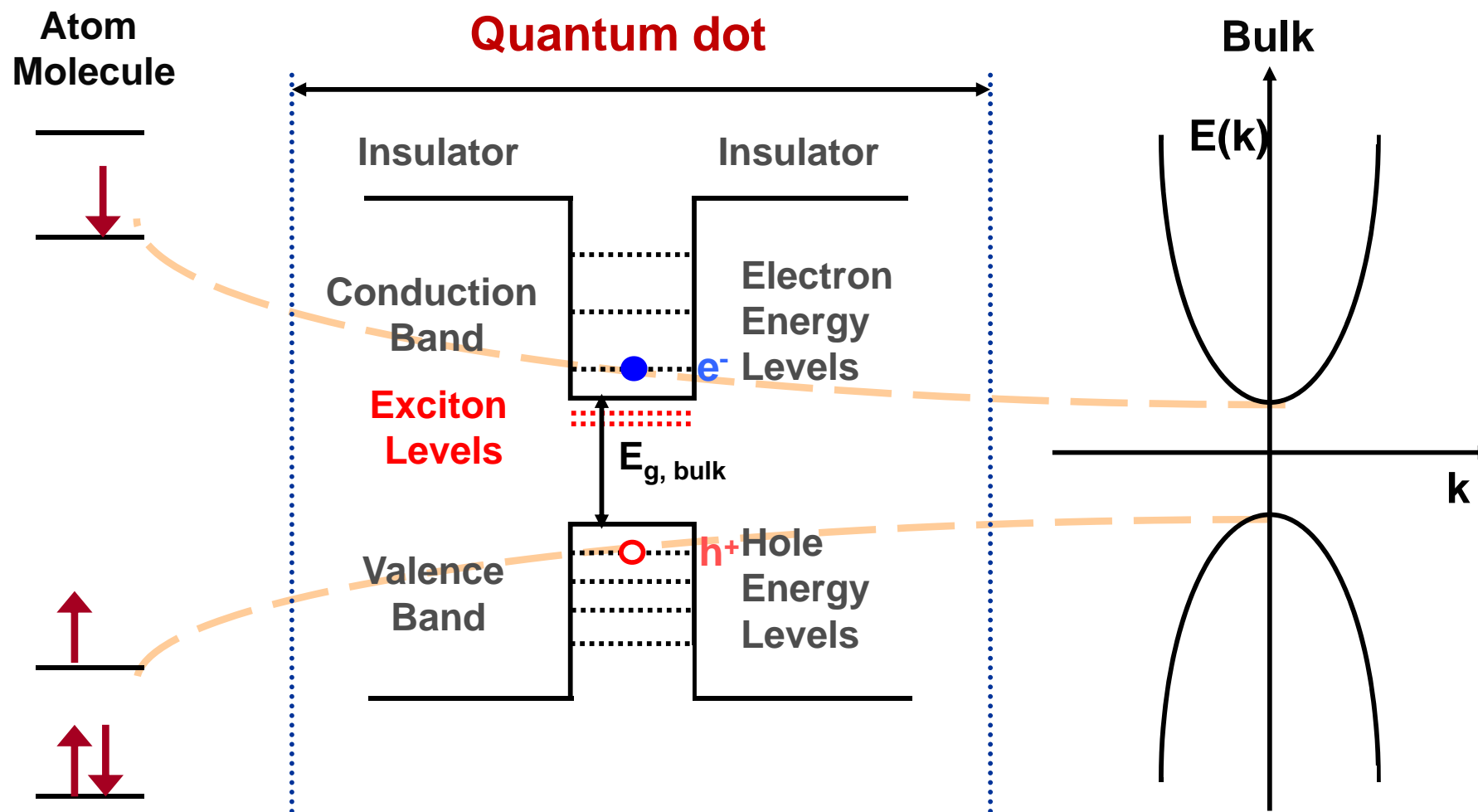
core emission wavelength
(size & composition)



shell surface passivation

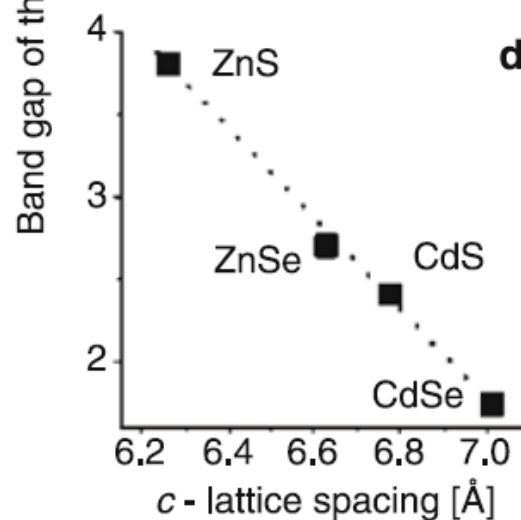
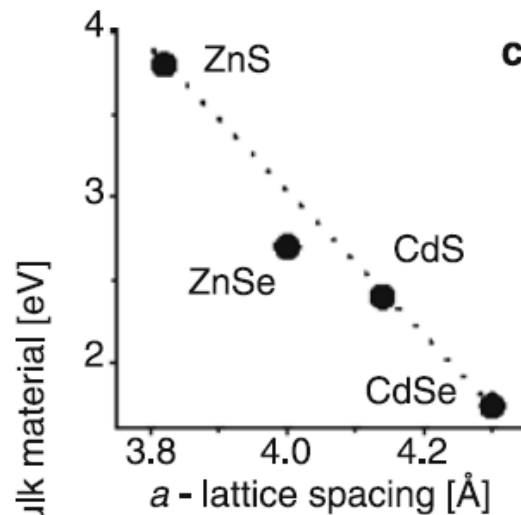
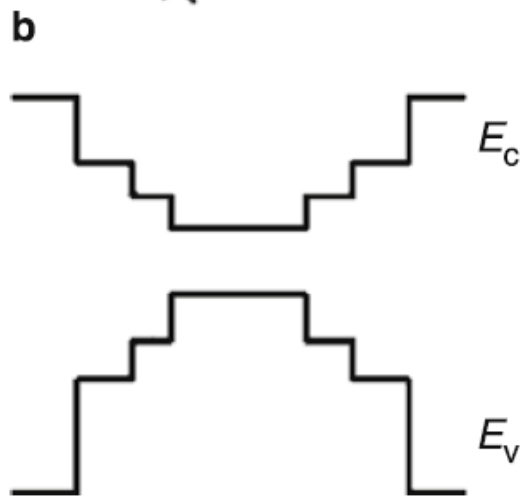
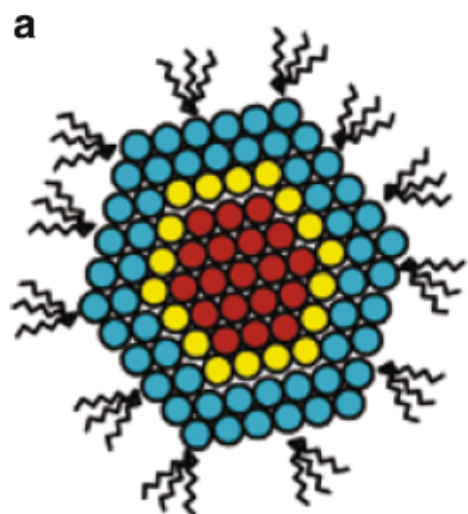
- Quantum dots have properties
 - High extinction coefficient
 - High electron mobility
 - Band gap & position tunability
 - Solution process capability
- Different methods to create quantum dots.
- Multiple applications: LEDs, LDs, Solar Cells, etc.

Energy structure of QDs

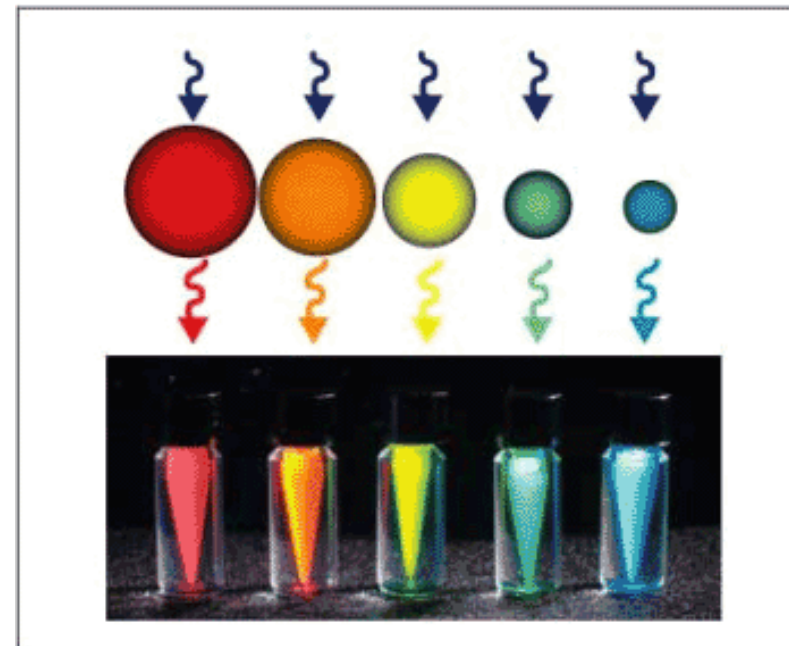


“Quantum dot is a nanometer-scale semiconductor crystallite which confines the electron-hole pair in all three dimensions.”

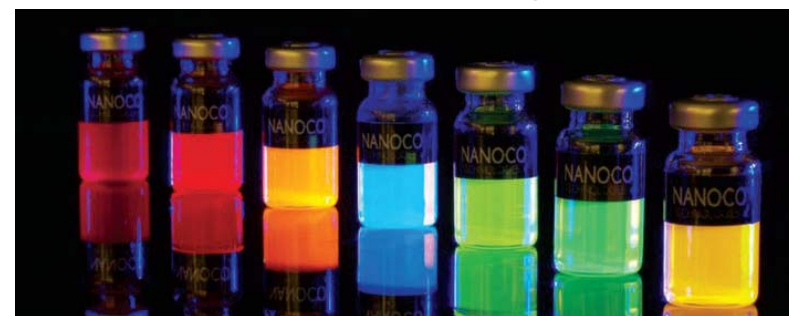
Energy band of QDs



Luminescence of CdSe QDs of different sizes



Quantum Dot Corp.



Core shell shell nanocrystal: **a** schematic outline and **b** the schematic energy level diagram; **c, d** relationship between band gap energy and lattice parameter of bulk wurzite phase CdSe, ZnSe, CdS, and ZnS

Dirk Dorfs, Alexander Eychmueller, "Multishell semiconductor nanocrystals", in Andrey L. Rogach (Ed.) Semiconductor Nanocrystal Quantum Dots, Synthesis, Assembly, Spectroscopy and Applications, Springer-Verlag/Wien, 2008.

Nanoparticle applications

- **Quantum dots**

- QDLEDs
- Solar cells
- Biomedicine

- **Magnetic nanoparticles**

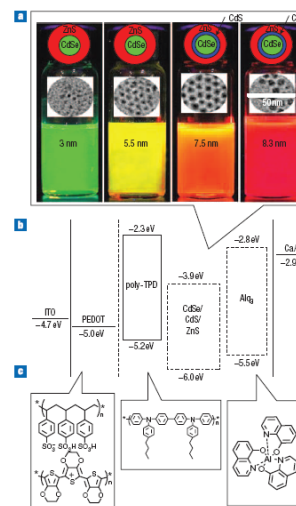
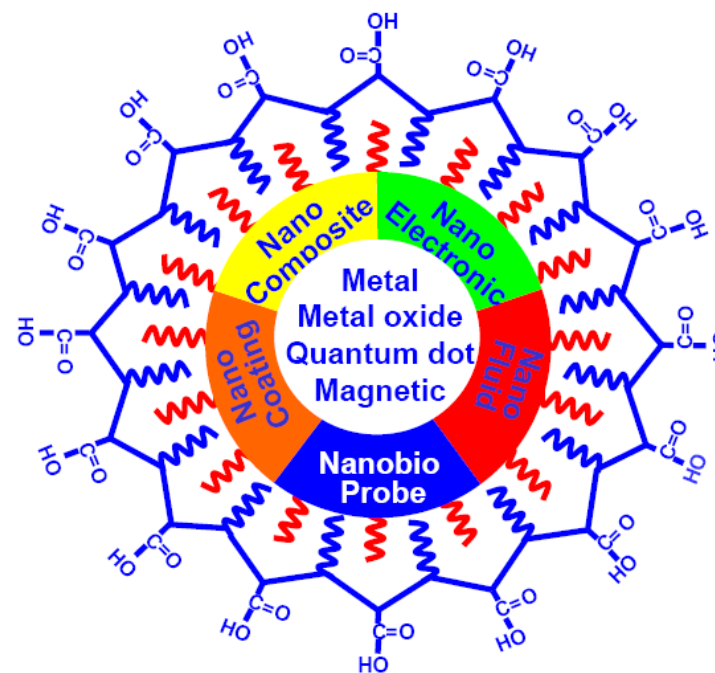
- Biomedicine: MRI. Hyperthermia, Drug delivery

- **Metal nanoparticles**

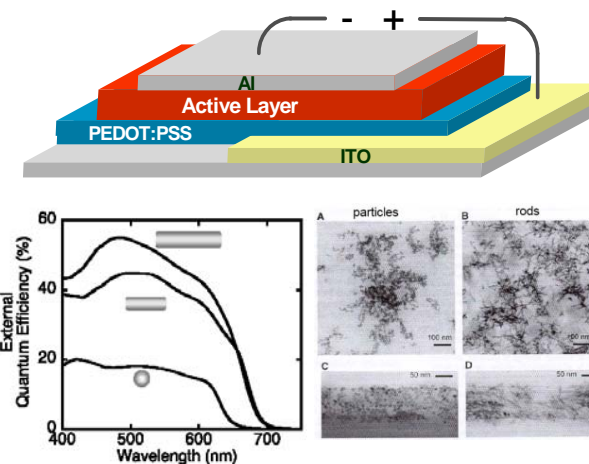
- Biodetection (Au, Ag)
- Electromagnetic shell (Fe, Ni, Co)
- Nanofluid

- **Metal oxide nanoparticles**

- Dielectrics
- Nanocomposite
- Nanocoating



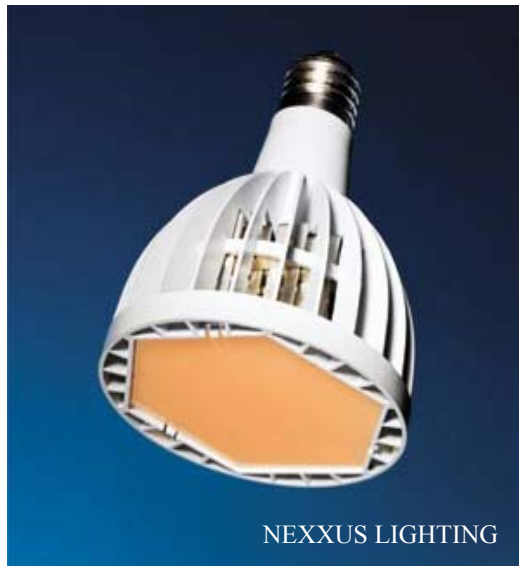
Q.-J Sun et al. (CAS, Ocean NanoTech),
Nature Photonics 1, 717 (2007)



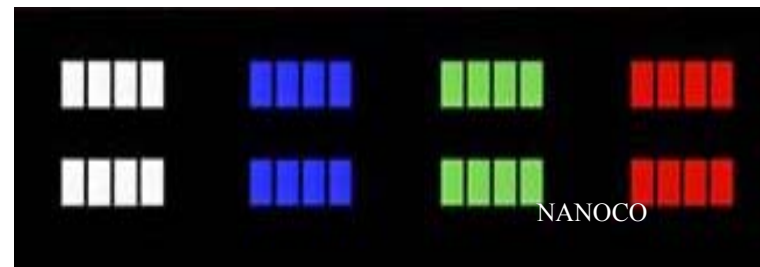
W. U. Huynh, J. J. Dittmer, A. P. Alivisatos,
Science, 295, 2425 (2002)

Examples of QD applications: LED, Lighting, Display

Lighting

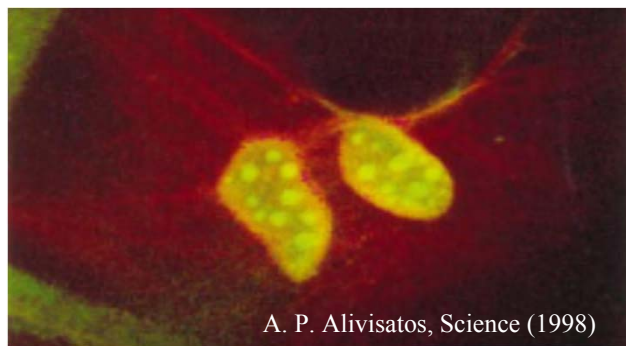
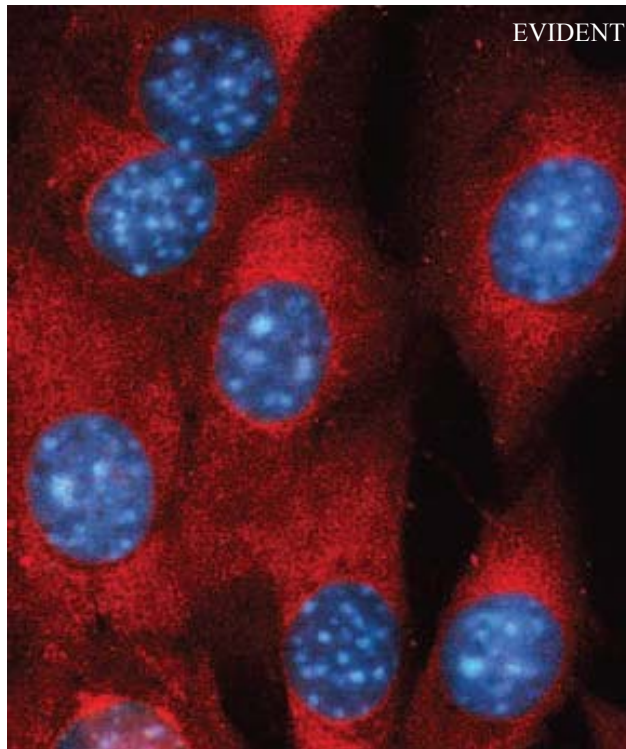


QLED & Display



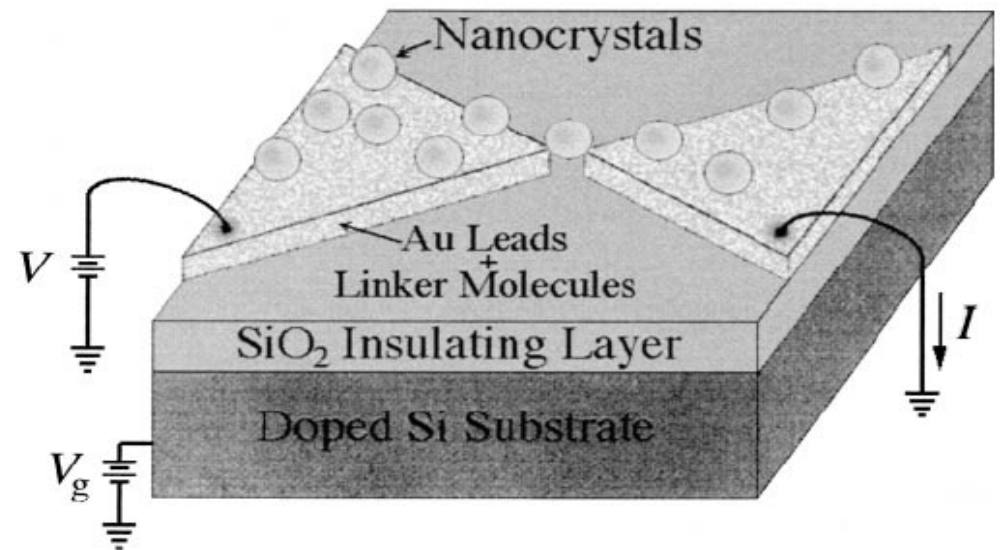
Other examples of QD applications

Bio-imaging



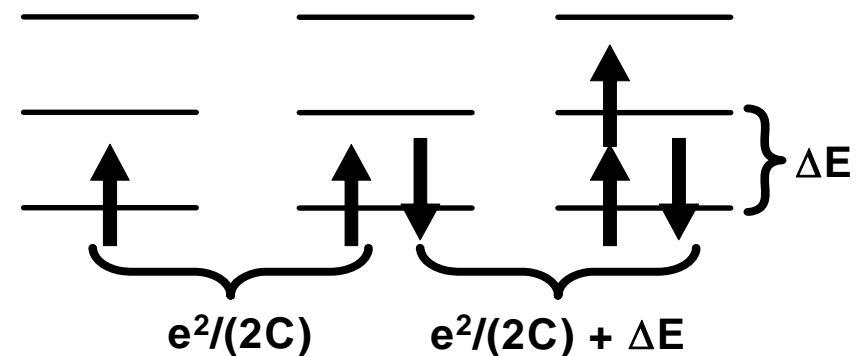
A. P. Alivisatos, *Science* (1998)

Single electron transistors



P. L. McEuen, *Nature* (1997)

Coulomb charging effect with limited DOS



*Basic quantum mechanics
applied to nanoclusters (QDs)*



Periodic Table

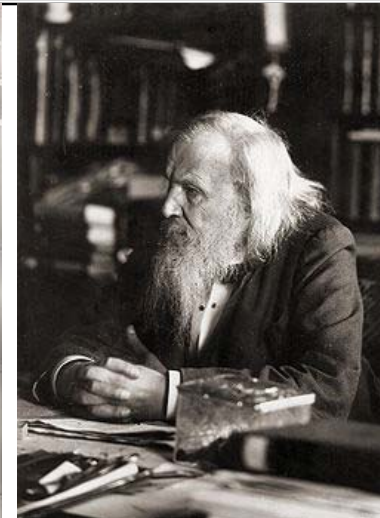
Table 7.2

The Periodic Table of the Elements

Group	1	2	Transition metals										3	4	5	6	7	8									
Period 1	1 H Hydrogen 1.008																	2 He Helium 4.003									
2	3 Li Lithium 6.941	4 Be Beryllium 9.012											5 B Boron 10.81	6 C Carbon 12.01	7 N Nitrogen 14.01	8 O Oxygen 16.00	9 F Fluorine 19.00	10 Ne Neon 20.18									
3	11 Na Sodium 22.99	12 Mg Magnesium 24.31											13 Al Aluminium 26.98	14 Si Silicon 28.09	15 P Phosphorus 30.97	16 S Sulfur 32.07	17 Cl Chlorine 35.45	18 Ar Argon 39.95									
4	19 K Potassium 39.10	20 Ca Calcium 40.08	21 Sc Scandium 44.96	22 Ti Titanium 47.88	23 V Vanadium 50.94	24 Cr Chromium 52.00	25 Mn Manganese 54.94	26 Fe Iron 55.8	27 Co Cobalt 58.93	28 Ni Nickel 58.69	29 Cu Copper 63.55	30 Zn Zinc 65.39	31 Ga Gallium 69.72	32 Ge Germanium 72.59	33 As Arsenic 74.92	34 Se Selenium 78.96	35 Br Bromine 79.90	36 Kr Krypton 83.80									
5	37 Rb Rubidium 85.47	38 Sr Strontium 87.62	39 Y Yttrium 88.91	40 Zr Zirconium 91.22	41 Nb Niobium 92.91	42 Mo Molybdenum 95.94	43 Tc Technetium (98)	44 Ru Ruthenium 101.1	45 Rh Rhodium 102.9	46 Pd Palladium 106.4	47 Ag Silver 107.9	48 Cd Cadmium 112.4	49 In Indium 114.8	50 Sn Tin 118.7	51 Sb Antimony 121.9	52 Te Tellurium 127.6	53 I Iodine 126.9	54 Xe Xenon 131.8									
6	55 Cs Cesium 132.9	56 Ba Barium 137.3											72 Hf Hafnium 178.5	73 Ta Tantalum 180.9	74 W Tungsten 183.9	75 Re Rhenium 186.2	76 Os Osmium 190.2	77 Ir Iridium 192.2	78 Pt Platinum 195.1	79 Au Gold 197.0	80 Hg Mercury 200.6	81 Tl Thallium 204.4	82 Pb Lead 207.2	83 Bi Bismuth 209.0	84 Po Polonium (209)	85 At Astatine (210)	86 Rn Radon (222)
7	87 Fr Francium (223)	88 Ra Radium 226.0											104 Rf Rutherfordium (261)	105 Db Dubnium (262)	106 Sg Seaborgium (263)	107 Ns Nobelium (262)	108 Hs Hassium (264)	109 Mt Meitnerium (266)	Halogens			Inert gases					
Alkali metals			Lanthanides (rare earths)																								
			57 La Lanthanum 138.9	58 Ce Cerium 140.1	59 Pr Praseodymium 140.9	60 Nd Neodymium 144.2	61 Pm Promethium (145)	62 Sm Samarium 150.4	63 Eu Europium 152.0	64 Gd Gadolinium 157.3	65 Tb Terbium 158.9	66 Dy Dysprosium 162.5	67 Ho Holmium 164.9	68 Er Erbium 167.3	69 Tm Thulium 168.9	70 Yb Ytterbium 173.0	71 Lu Lutetium 175.0										
			89 Ac Actinium (227)	90 Th Thorium 232.0	91 Pa Protactinium 231.0	92 U Uranium 238.0	93 Np Neptunium (237)	94 Pu Plutonium (244)	95 Am Americium (243)	96 Cm Curium (247)	97 Bk Berkelium (247)	98 Cf Californium (251)	99 Es Einsteinium (252)	100 Fm Fermium (257)	101 Md Mendelevium (260)	102 No Nobelium (259)	103 Lw Lawrencium (262)										
			Actinides																								

The number above the symbol of each element is its atomic number, and the number below its name is its average atomic mass. The elements whose atomic masses are given in parentheses do not occur in nature but have been created in nuclear reactions. The atomic mass in such a case is the mass number of the most long-lived radioisotope of the element.

Elements with atomic numbers 110, 111, 112, 114, and 116 have also been created but not yet named.



Dmitri Ivanovich Mendeleev

(1834.2.8 –1907.2.2)
In 1869, he invented the table to illustrate recurring ("periodic") trends in the properties of the elements.

A. Beiser, Concepts of Modern Physics, 6th ed., McGraw-Hill, New York, USA, 2003.



Schrödinger equation

Time-dependent Schrödinger equation

$$i\hbar \frac{\partial}{\partial t} \Psi = \hat{H}\Psi$$

$$\hat{H} = -\frac{\hbar^2}{2m} \nabla^2 + U$$

$$\Psi(x, t) = \psi e^{-(iE/\hbar)t}$$

Time-independent Schrödinger equation

$$\hat{H}\psi_n = E_n\psi_n$$

Steady-state Schrödinger equation in 1-dim.

$$-\frac{\hbar^2}{2m} \frac{\partial^2 \psi}{\partial x^2} + U\psi = E\psi$$

Boundary condition \rightarrow energy quantization.



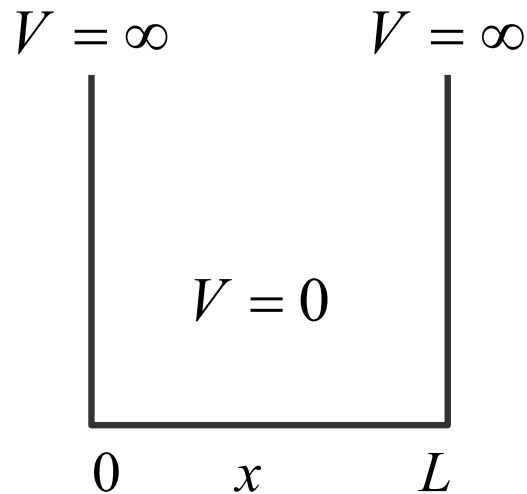
Erwin Schrödinger
(1887. 8. 12 -1961. 1. 4)
Nobel Prize in Physics (1933)



Erwin Schrödinger 의 대표적 논문

- **Schrödinger Eq., Energy eigenvalues for the hydrogen-like atom**
E. Schrödinger, Quantisierung als Eigenwertproblem (Quantization as an Eigenvalue Problem), Ann. Phys. 1926, vol. 384, 361–376
- **Quantum harmonic oscillator, the rigid rotor and the diatomic molecule, New derivation of the Schrödinger equation**
E. Schrödinger, Quantisierung als Eigenwertproblem, Ann. Phys. 1926, vol. 384, 489–527
- **Equivalence of Schrödinger approach to that of Heisenberg, Treatment of the Stark effect**
E. Schrödinger, Über das Verhältnis der Heisenberg-Born-Jordanschen Quantenmechanik zu der meinem, Ann. Phys. 1926, vol. 384, 734–756
- **Treat problems in which the system changes with time, as in scattering problems**
E. Schrödinger, Quantisierung als Eigenwertproblem, Ann. Phys. 1926, vol. 385, 437–490
- E. Schrödinger, Quantisierung als Eigenwertproblem, Ann. Phys. 1926, vol. 386, 109–139
- E. Schrödinger, Der stetige Übergang von der Mikro-zur Makromechanik, Die Naturwissenschaften, 14. Jahrg. Heft 28, S. 664–666 (1926).

Schrödinger equation: Particle in a box



Within the box $V=0$.
$$\frac{\partial^2 \psi}{\partial x^2} + \frac{2m}{\hbar^2} E \psi = 0$$

Wave functions
$$\psi_n = A \sin \frac{\sqrt{2mE}}{\hbar} x + B \cos \frac{\sqrt{2mE}}{\hbar} x$$

Boundary condition: $\psi=0$ at $x=0$ and a .

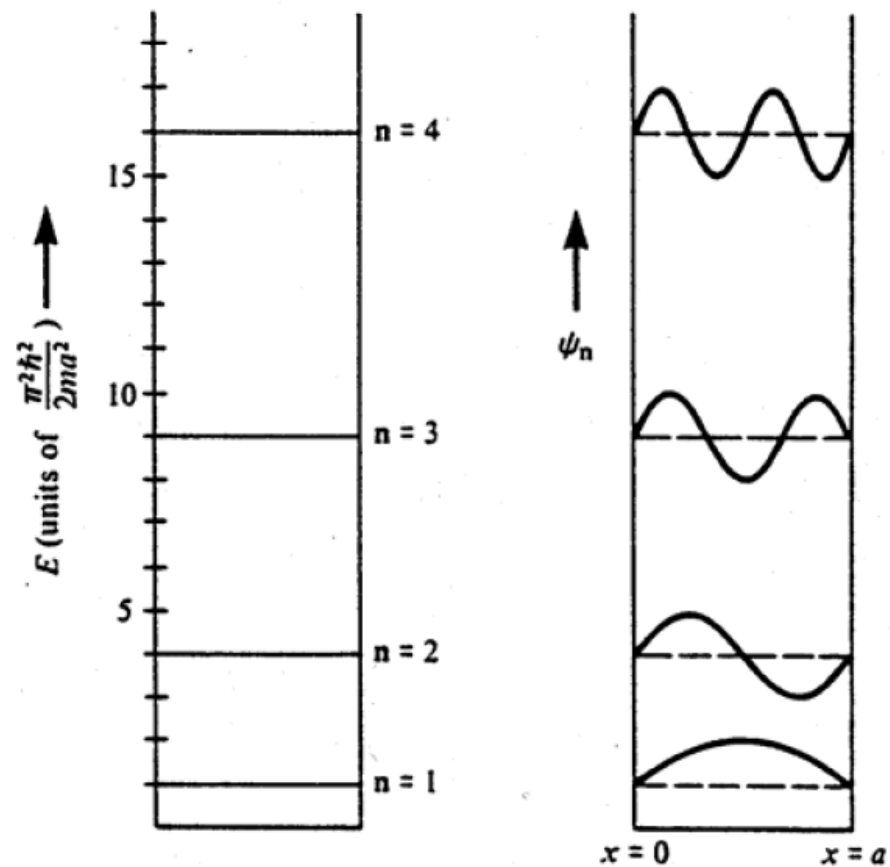
$$B = 0, \quad \frac{\sqrt{2mE}}{\hbar} L = n\pi, \quad n = 1, 2, 3, \dots$$

Energy levels for a particle in a box

$$E_n = \frac{\hbar^2}{2m} \left(\frac{n\pi}{L} \right)^2 = \frac{n^2 \pi^2 \hbar^2}{2mL^2}, \quad n = 1, 2, 3, \dots$$

Wave functions for a particle in a box

$$\psi_n = \sqrt{\frac{2}{L}} \sin \frac{n\pi x}{L}$$

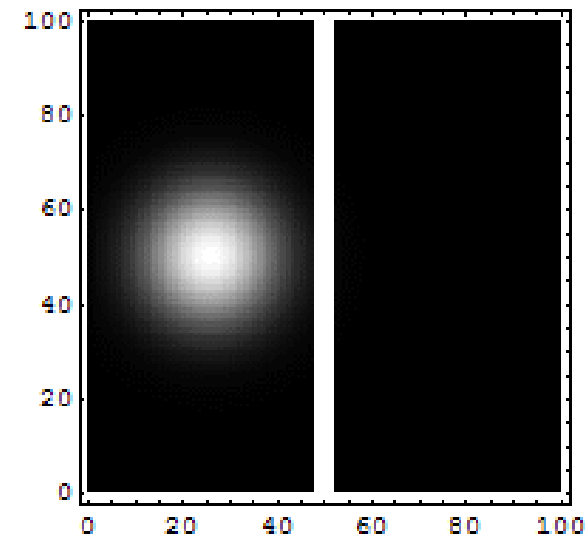
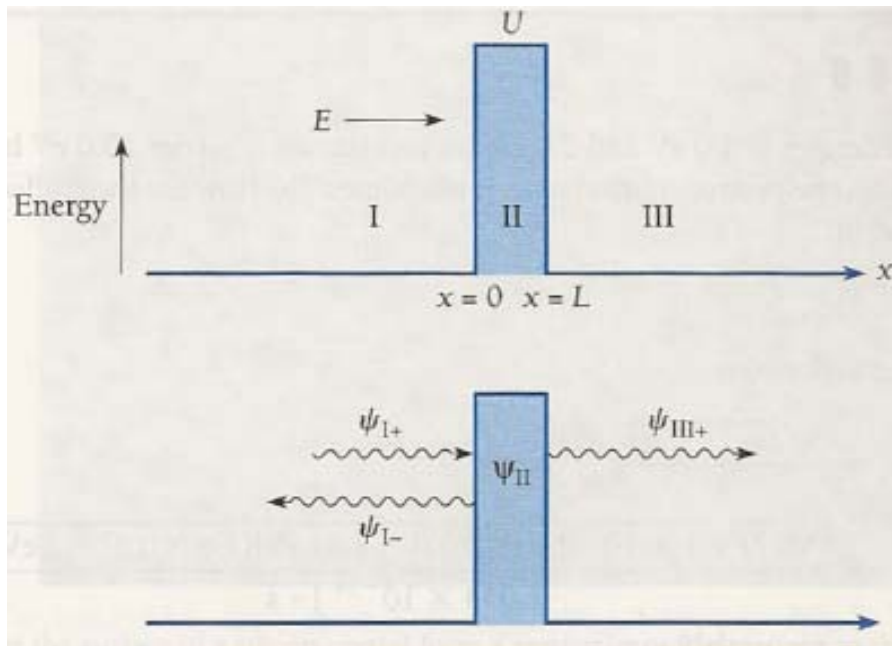


Schrödinger equation: Tunnel effect

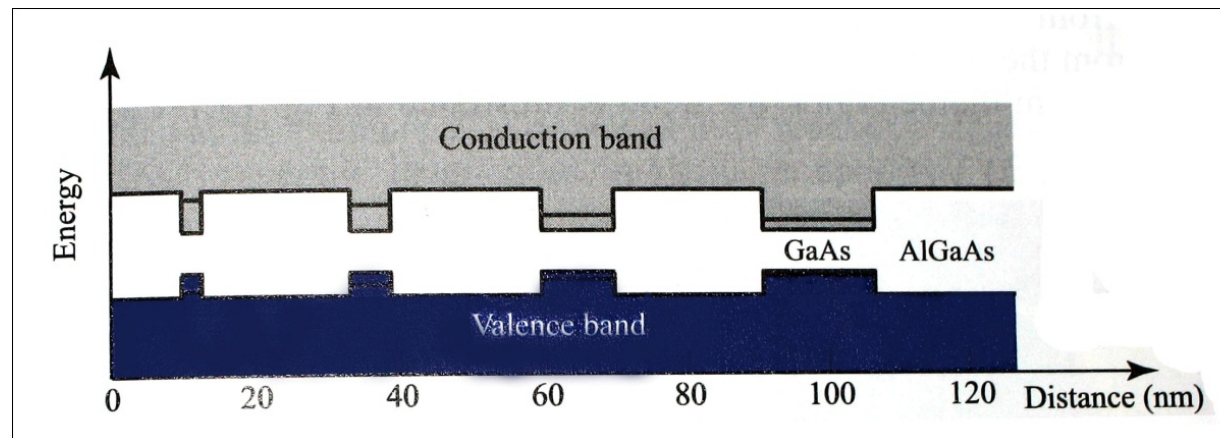
For $E < U$, the particle has a certain probability - not necessarily great, but not zero either-of passing through the barrier and emerging on the other side.

Approximate transmission probability

$$T = e^{-2k_2L}, \quad k_2 = \frac{\sqrt{2m(U - E)}}{\hbar}$$



Reflection and tunnelling of an electron wavepacket directed at a potential barrier.
http://en.wikipedia.org/wiki/Quantum_tunneling



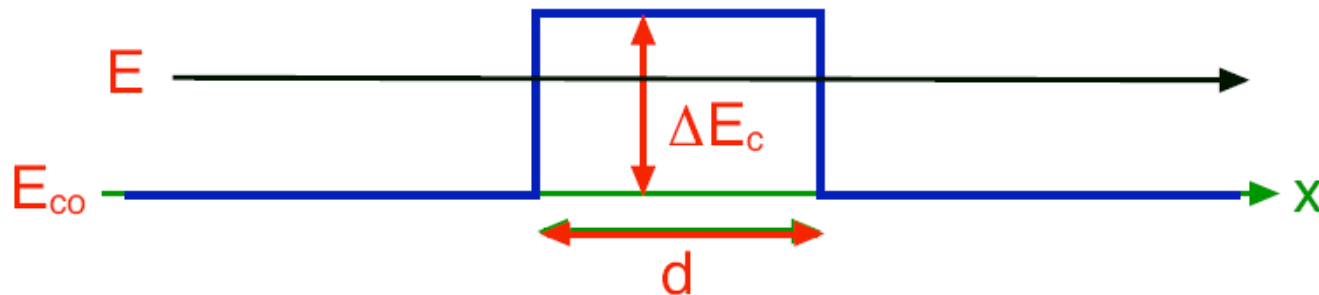
B.E.A. Saleh, M.C. Teich. Fundamentals of Photonics. Fig. 13.1-11.

A. Beiser, Concepts of Modern Physics, 6th ed., McGraw-Hill, New York, USA, 2003, Chapter 3



Transmission probabilities

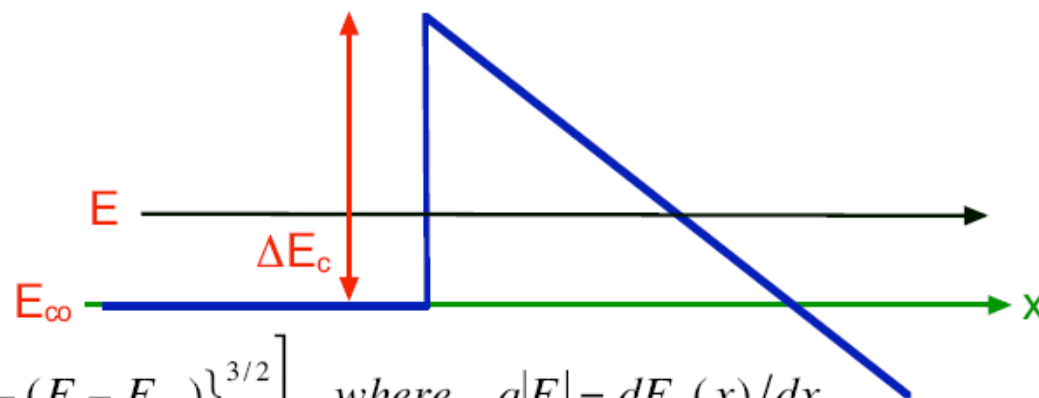
Rectangular barrier



$$T = 4 / \left\{ 4 \cosh^2 \alpha d + [(\alpha / k) - (k / \alpha)] 2 \sinh^2 \alpha d \right\}$$

where $k^2 = 2m^*(E - E_c) / \hbar^2$ and $\alpha^2 = 2m_o[\Delta E_c - (E - E_c)] / \hbar^2$

Triangular barrier:



$$T = \exp \left[\frac{-4(2m^*)^{1/2}}{3qF\hbar} \left\{ \Delta E_c - (E - E_{co}) \right\}^{3/2} \right] \quad \text{where } q|F| = dE_c(x)/dx$$



Finite potential well

$$\psi_{II} = \begin{cases} A \cos kx & \text{(symmetric solutions)} \\ A \sin kx & \text{(antysymmetric solutions)} \end{cases}$$

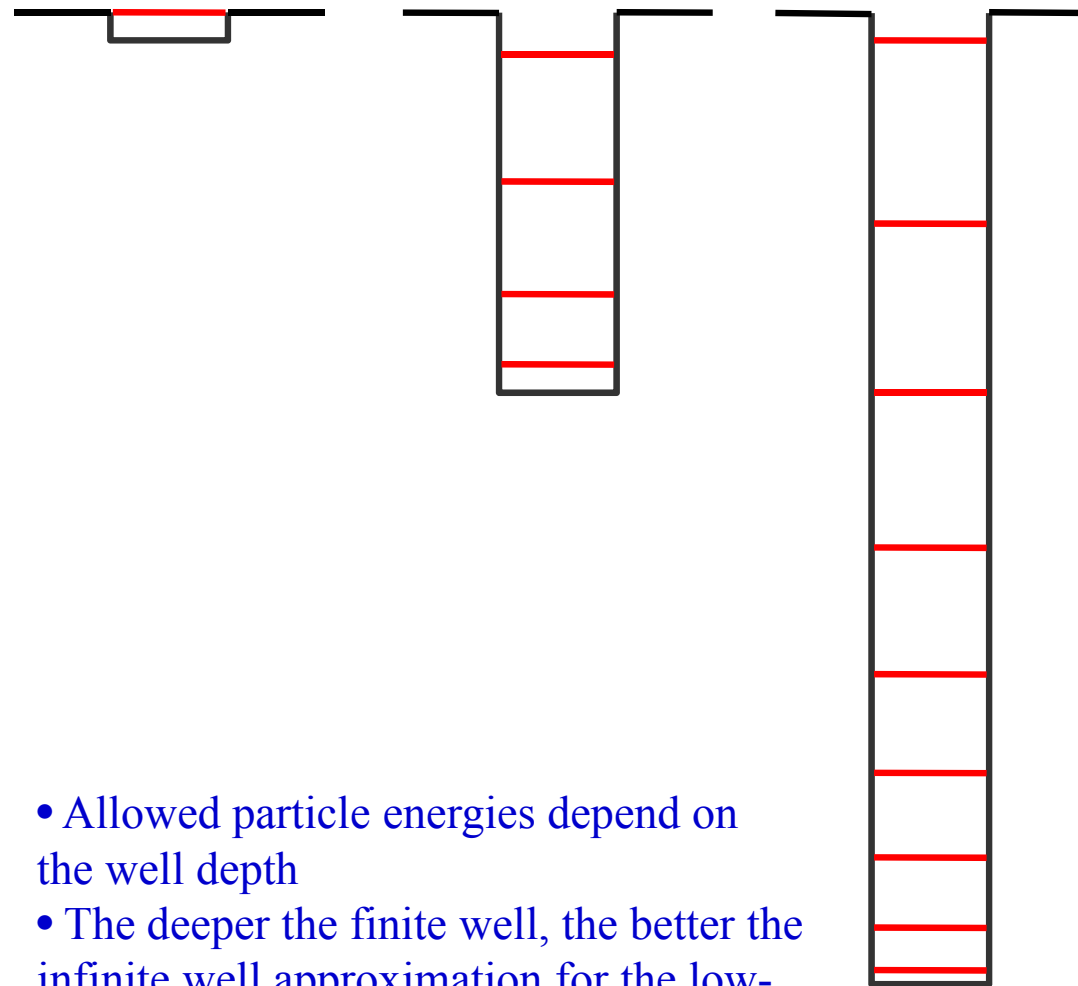
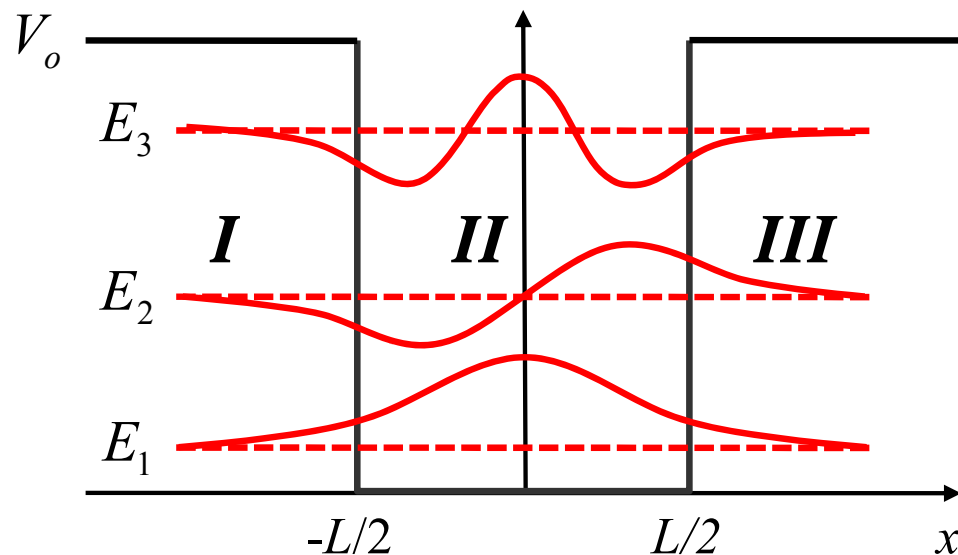
$$\psi_I = Be^{\gamma x} \quad k^2 = 2mE / \hbar^2$$

$$\psi_{III} = Be^{-\gamma x} \quad \gamma^2 = 2m(V_o - E) / \hbar^2$$

Boundary conditions; $\psi_I(-\frac{L}{2}) = \psi_{II}(-\frac{L}{2}); \frac{d\psi_I}{dx}(-\frac{L}{2}) = \frac{d\psi_{II}}{dx}(-\frac{L}{2});$
 $\psi_{II}(\frac{L}{2}) = \psi_{III}(\frac{L}{2}); \frac{d\psi_{II}}{dx}(\frac{L}{2}) = \frac{d\psi_{III}}{dx}(\frac{L}{2})$

$$k \tan \frac{kL}{2} = \gamma \quad \text{(symmetric solutions)}$$

$$k \tan\left(\frac{kL}{2} - \frac{\pi}{2}\right) = \gamma \quad \text{(antysymmetric solutions)}$$

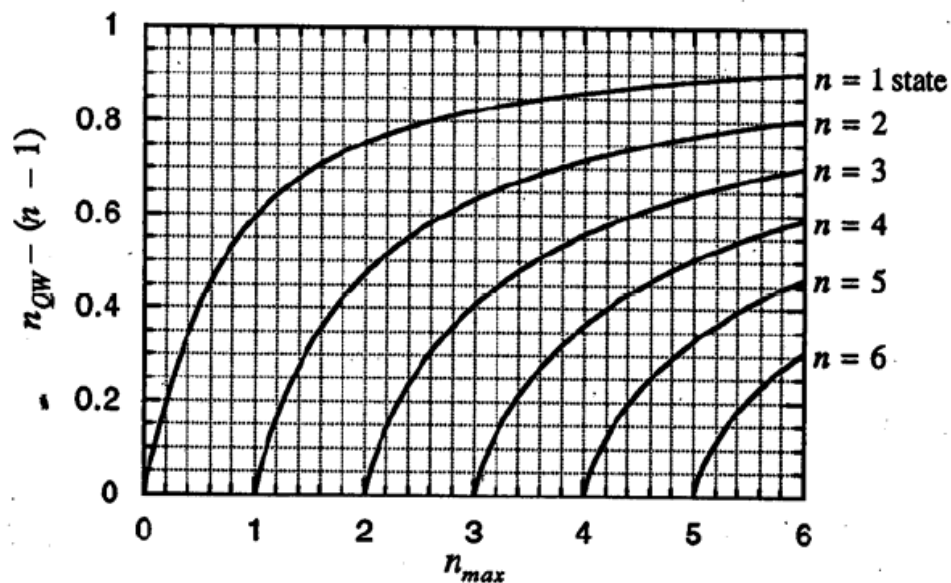


- Allowed particle energies depend on the well depth
- The deeper the finite well, the better the infinite well approximation for the low-lying energy values
- Small L \rightarrow larger energy level separation



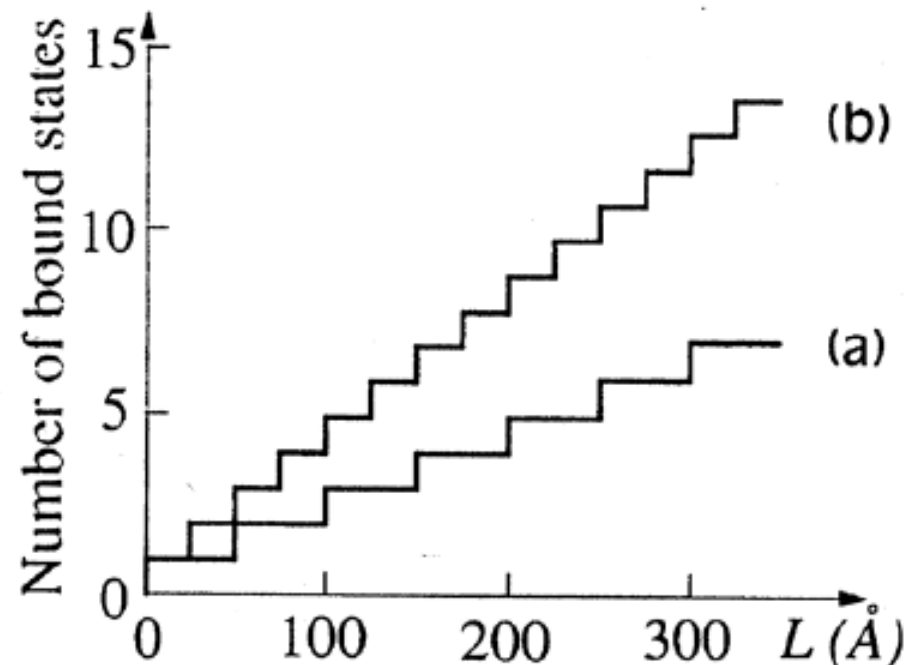
Bound states as a function of well thickness

$$n_{\max} = 1 + \text{Int} \left[\sqrt{\frac{2m^* V_0 L^2}{\pi^2 \hbar^2}} \right]$$



Plot of quantum numbers as a function of the maximum allowed quantum number which is determined by the potential height V_0

Figure 3.5. The number of the bound states of a square well plotted as a function of well thickness: (a) $V_b = 224$ meV, $m^* = 0.067$ m; (b) $V_b = 150$ meV, $m^* = 0.4$ m. [After G. Bastard, *Wave Mechanics Applied to Semiconductor Heterostructures* (Halsted, New York, 1988).]



Density of states (DOS)

- Density of states (DoS)
 - e.g. in 3D (bulk material):

Volume in k-space per state: $\left(\frac{2\pi}{L}\right)^3$

Volume in k-space occupied by states with energy less than E :

$$V_k = \frac{4\pi}{3} k^3, \quad k = \frac{\sqrt{2m(E - E_c)}}{\hbar}$$

Number of electron states in this volume:

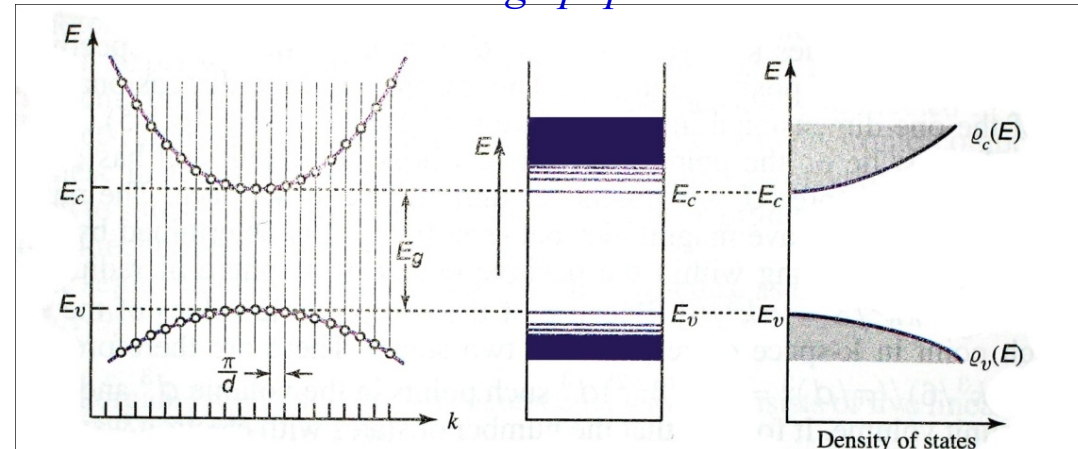
$$N(E) = 2 \cdot \frac{4\pi k^3 / 3}{(2\pi / L)^3} = \frac{L^3}{3\pi^2} \left(\frac{2m}{\hbar}\right)^{3/2} (E - E_c)^{3/2}$$

Density of states with energies between E and $E+dE$ per unit volume:

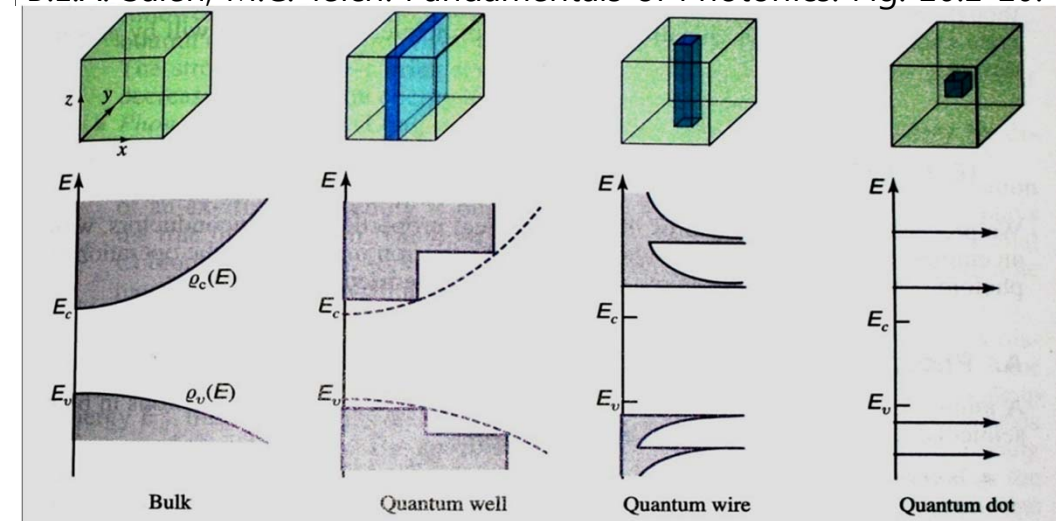
$$g(E) = \frac{1}{L^3} \frac{dN(E)}{dE} = \frac{1}{2\pi^2} \left(\frac{2m}{\hbar}\right)^{3/2} (E - E_c)^{1/2}$$

Lower the dimension greater the density of states near the band edge

→ Greater proportion of the injected carriers contribute to the band edge population.



B.E.A. Saleh, M.C. Teich. Fundamentals of Photonics. Fig. 16.1-10.



B.E.A. Saleh, M.C. Teich. Fundamentals of Photonics. Fig. 16.1-29.



Optical Excitation

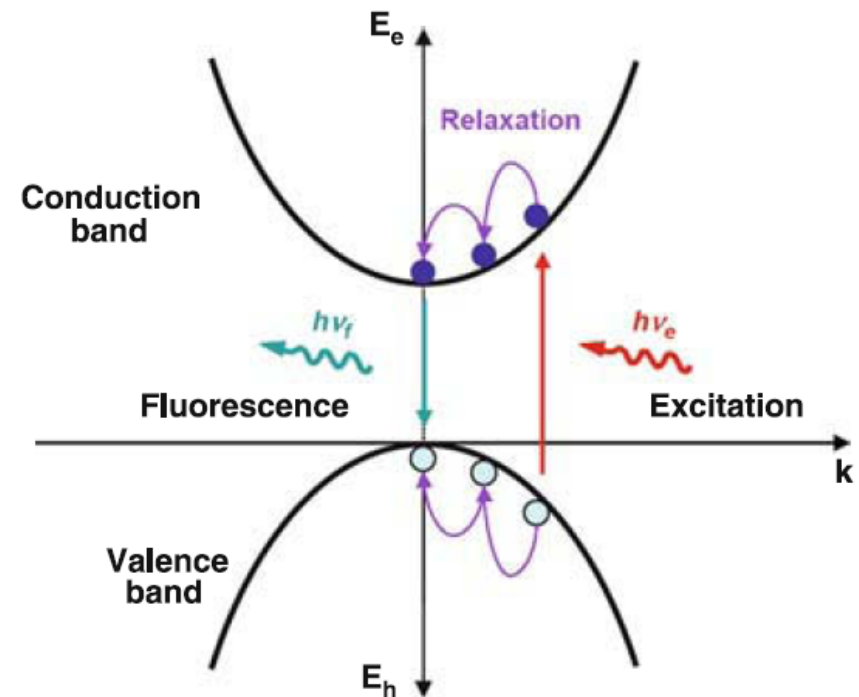
- Exciton: bound electron-hole pair
- Excite semiconductor \rightarrow creation of e-h pair
 - There is an attractive potential between electron and hole
 - $m_h^* > m_e^* \rightarrow$ hydrogen-like system
 - Binding energy determined from Bohr Theory
- In QDs, excitons are generated inside the dot
- Excitons are confined to the dot
 - Degree of confinement is determined by dot size
 - Discrete energies
- Exciton absorption \Rightarrow δ -function-like peaks in absorption

Orbit radii in the Bohr atom

$$r_n = \frac{n^2 h^2 \epsilon_o}{\pi m e^2} = a_o n^2 \quad n = 1, 2, 3, \dots$$

Energy levels

$$E_n = -\frac{e^2}{8\pi\epsilon_o r_n} = -\frac{m e^4}{8\epsilon_o^2 h^2} \left(\frac{1}{n^2}\right) \quad n = 1, 2, 3, \dots$$



Optical absorption and PL of quantum wells

- Properties determined by the size of quantum wells
- Smaller size → larger energy band gap → shorter wavelength

$$E_i^C - E_i^V = \left(E^C + \frac{\pi^2 \hbar^2 n_i^2}{2m_e^* L^2} \right) - \left(E^V - \frac{\pi^2 \hbar^2 n_i^2}{2m_h^* L^2} \right) = E_g + \frac{\pi^2 \hbar^2 n_i^2}{2L^2} \left(\frac{1}{m_e^*} + \frac{1}{m_h^*} \right)$$

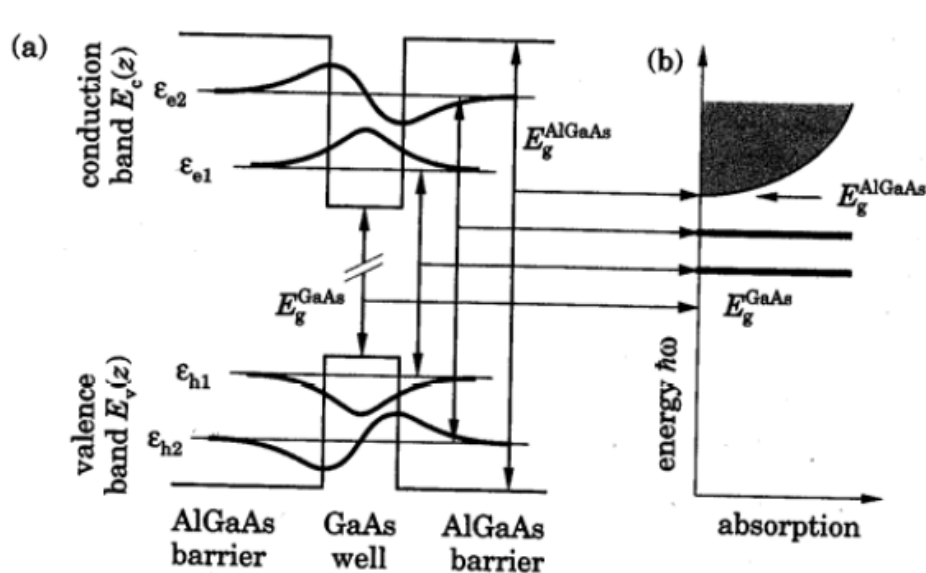


FIGURE 1.3. Optical absorption in a quantum well formed by a layer of GaAs surrounded by AlGaAs. (a) Potential well in conduction and valence band, showing two bound states in each; the energy gap of GaAs is really much larger than this diagram implies. (b) Transitions between states in the quantum well produce absorption lines between the band gaps of the GaAs well and AlGaAs barrier.

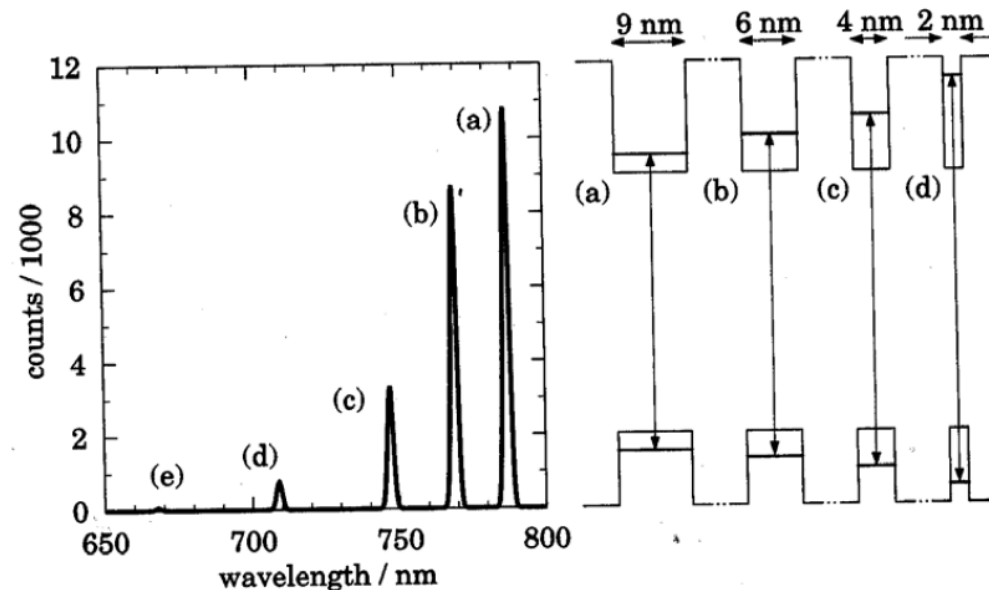


FIGURE 1.4. Photoluminescence as a function of wavelength for a sample with four quantum wells of different widths, whose conduction and valence bands are shown on the right. The barriers between the wells are much thicker than drawn. [Data kindly supplied by Prof. E. L. Hu, University of California at Santa Barbara.]

Basic properties of Quantum wells and dots



Energy levels of QDs

Very small semiconductor particles with a size comparable to the Bohr radius of the excitons (separation of electron and hole).

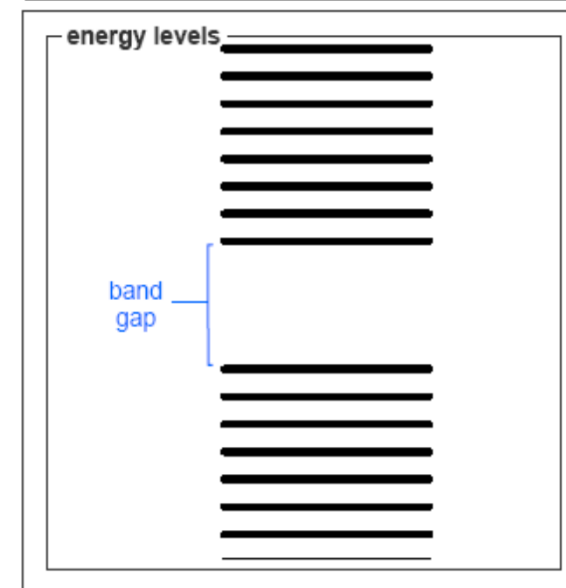
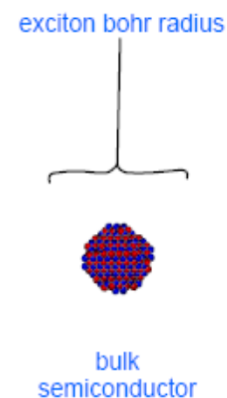
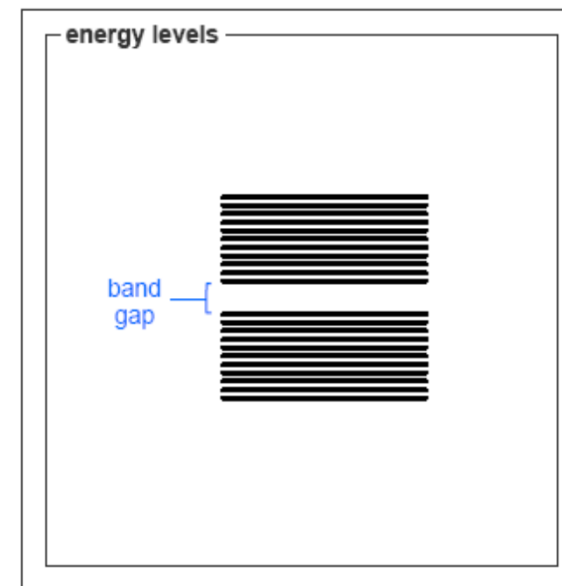
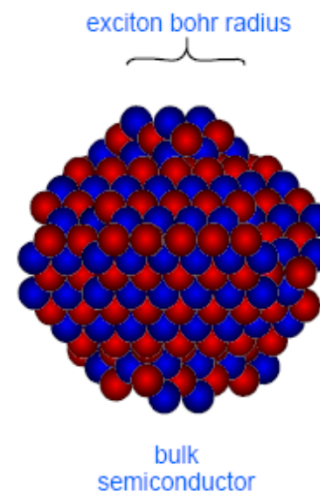
- Typical dimensions: 1 – 10 nm
- Different shapes (cubes, spheres, pyramids, etc.)
- The optical and electronic properties of QDs can be controlled by their size, shape, and composition.

CdSe Quantum Dot

- 5 nm dots: red
- 1.5 nm dots: violet



B.E.A. Saleh, M.C. Teich. Fundamentals of Photonics. Fig. 13.1-12.



From <http://www.evidenttech.com/quantum-dots-explained/how-quantum-dots-work.html> (Evident Technologies. 2010).

Small enough to see quantum effect

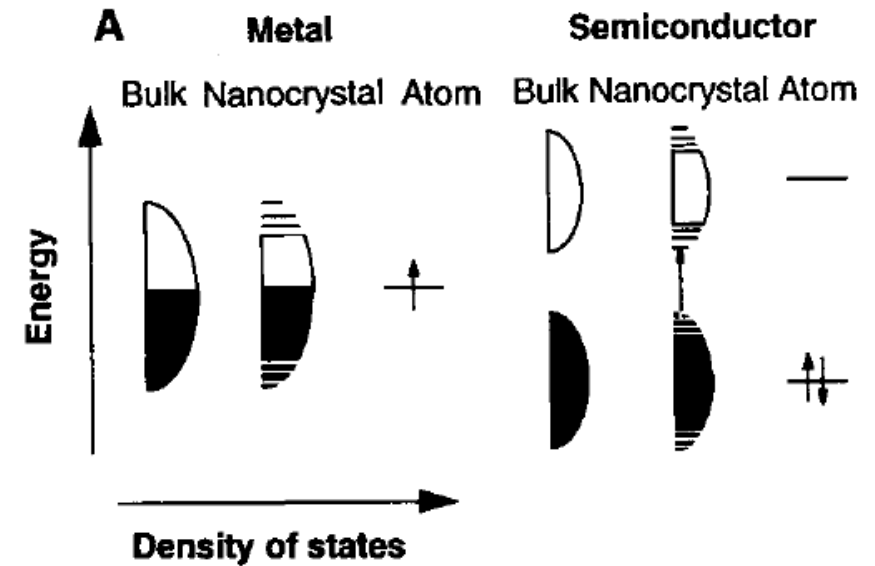
In order to see quantum effect, energy levels must be sufficiently separated to remain distinguishable under broadening (e.g. thermal).

For free electrons, $\lambda \sim 6$ nm (at 300 K).

$$\frac{\hbar^2 k^2}{2m} = \frac{3}{2} k_B T; \quad \lambda = \frac{h}{\sqrt{3mk_B T}} = \frac{6.626 \times 10^{-34}}{\sqrt{3 \cdot 9.1 \times 10^{-31} \cdot 1.38 \times 10^{-23} \cdot 300}} \approx 6 \text{ nm}$$

In semiconductors, this condition can be realized for a given temperature at a relatively large size compared to metals, insulators, or molecular crystals.

- **In metal:**
 - Energy level spacing at the Fermi energy E_F is very small.
- **In semiconductors:**
 - Effective mass $m^* \sim 0.1 m$
 - E_F lies between two bands, such that the edges of the bands dominate the low-energy optical and electrical behavior.
 - Quantum effects occurs on size of clusters of $L \sim 10$ nm (10,000 atoms)
- **In molecular crystals:**
 - Narrow band width due to weak van der Waals interaction
 - not much size variation in optical or electrical properties.



A. P. Alivisatos, Science 271, 933 (1996).

Size matters

In a material of a single chemical composition, fundamental properties of materials can be changed by the controlling the size of nanoclusters (QDs).

- Energy band gap
- Electrical transport
- Melting temperature
- etc..

TABLE I. Electronic parameters for the indicated crystalline direct gap semiconductors, ϵ is the dielectric coefficient at optical frequencies. The effective masses are in units of the free electron mass. E_g is the band gap.

	$E_g(0\text{ K})$ (eV)	m_e^*	m_h^*	ϵ
InSb	0.24	0.015	0.39	15.6
GaAs	1.52	0.07	0.68	10.9
CdS	2.58	0.19	0.8	5.7
ZnO	3.44	0.24	0.45	3.7

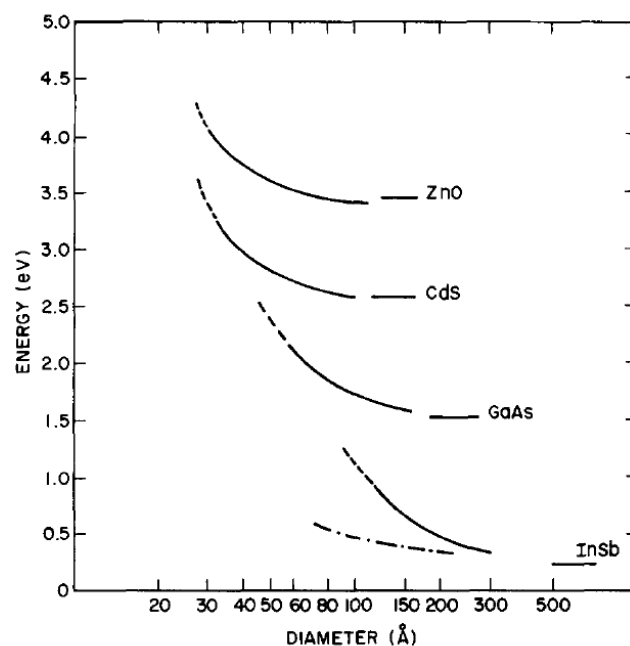
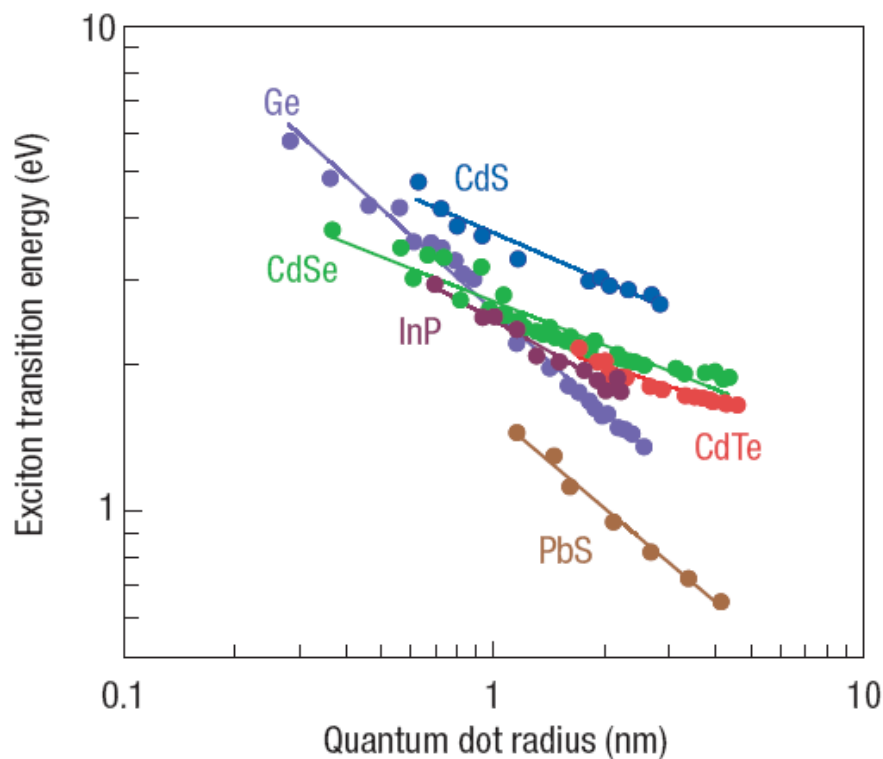


FIG. 1. Energy of the lowest excited electronic state as a function of crystal-lite diameter, as calculated via wave function (13). Short horizontal solid lines are the bulk band gap energies of the indicated materials. Dot-dashed line for InSb incorporates surface carrier charge density as described in the text.

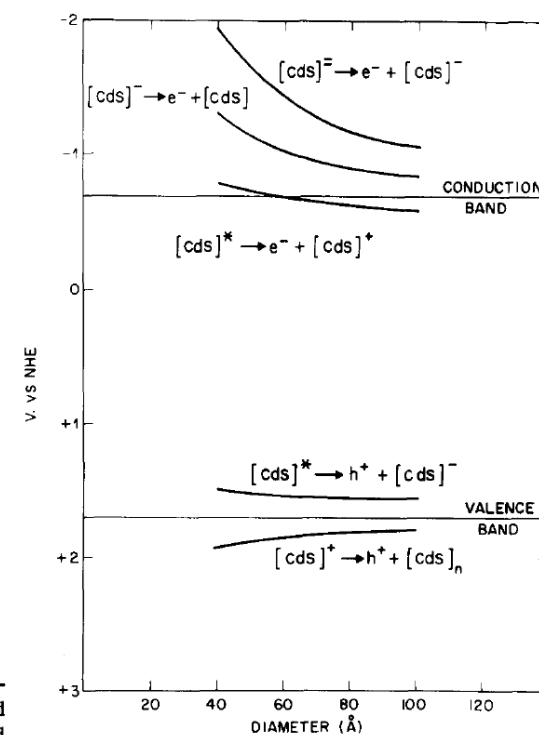


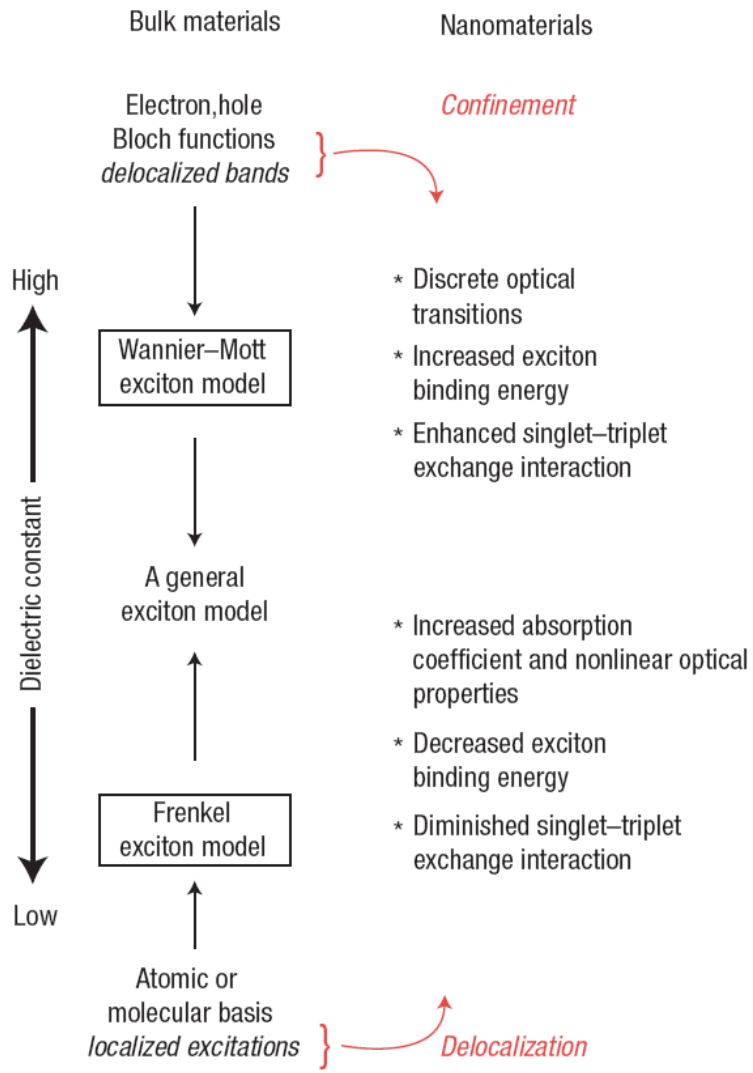
FIG. 2. Calculated size dependence of the indicated redox processes.

G. D. Scholes, G. Rumbles, Nature Materials 5, 683 (2006)

L. E. Brus, J. Chem. Phys. 80, 4403 (1984)



Quantum confinement effects



- Nanomaterials**
- Confinement*
- * Discrete optical transitions
 - * Increased exciton binding energy
 - * Enhanced singlet-triplet exchange interaction
- Bulk materials**
- * Increased absorption coefficient and nonlinear optical properties
 - * Decreased exciton binding energy
 - * Diminished singlet-triplet exchange interaction
- Delocalization*

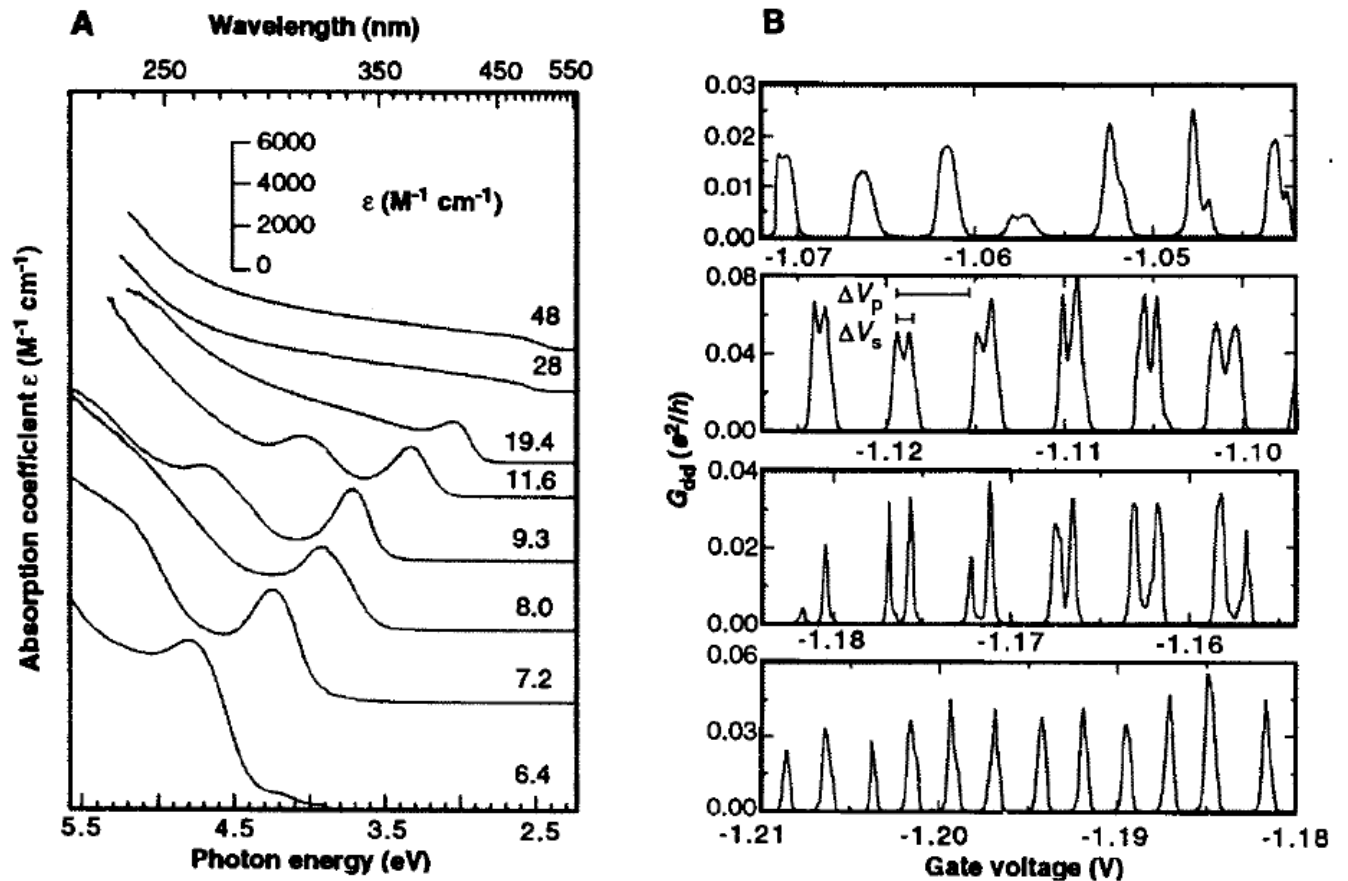


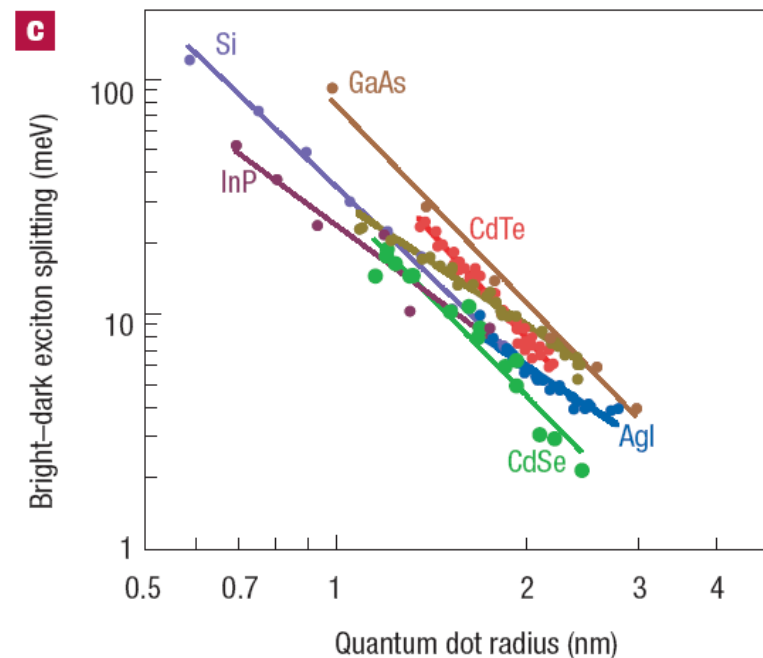
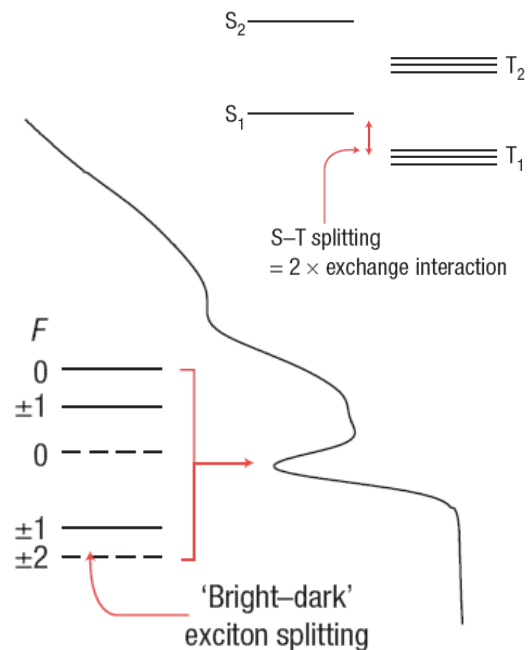
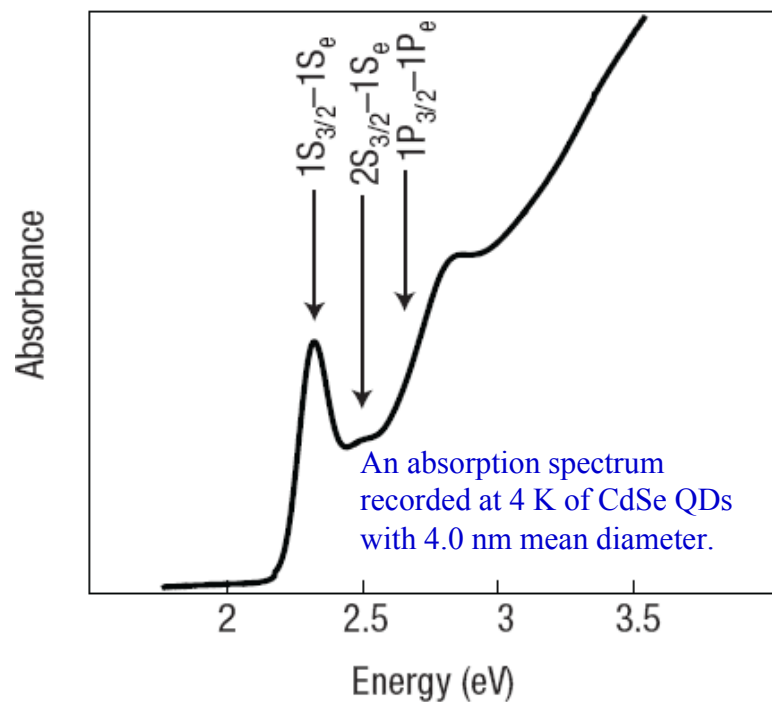
Fig. 3. (A) Quantum confinement effects on the absorption spectra of CdS nanocrystal quantum dots. With reduced size, the spectra shift to higher energy and the oscillator strength is concentrated into a small number of transitions. [Reprinted from (2) with permission] (B) Variations in the conductance G_{dc} versus gate voltage for two coupled GaAs quantum dots, as a function of the interdot coupling. V_d , drain voltage; V_s , source voltage. [Reprinted from (23) with permission]

G. D. Scholes, G. Rumbles, Nature Materials 5, 683 (2006)

A. P. Alivisatos, Science 271, 933 (1996.)



Electronic transition in colloidal CdSe quantum dots

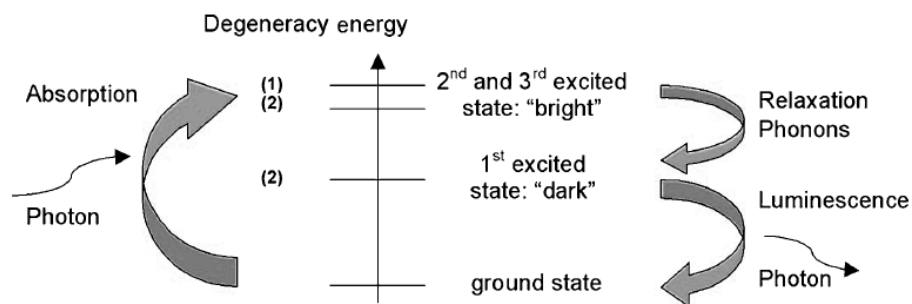


Hole and electron states associated with excitons seen as the prominent absorption features are labelled according to the assignments of ref. [A. I. Ekimov, *et al.*, J. Opt. Soc. Am. B **10**, 100 (1993)]. That notation specifies a hole or electron state as $n^*(l, l+2)F$, where n^* labels ground and excited states, l is the minimum orbital quantum number and $F = l + j$ is the total angular momentum quantum number (orbital plus spin), containing F_z from $-F$ to $+F$. Usually just the major contributor out of l or $l + 2$, or alternatively just l , is written as S, P, D and so on. That quantum number is associated with the envelope function, usually modelled mathematically as a spherical Bessel function $j_l(x)$. The quantum number j is associated with the Bloch function. For example, the upper valence band of a zinc blende structure has $j = 3/2$ and $j_z = -3/2, -1/2, 1/2, 3/2$.

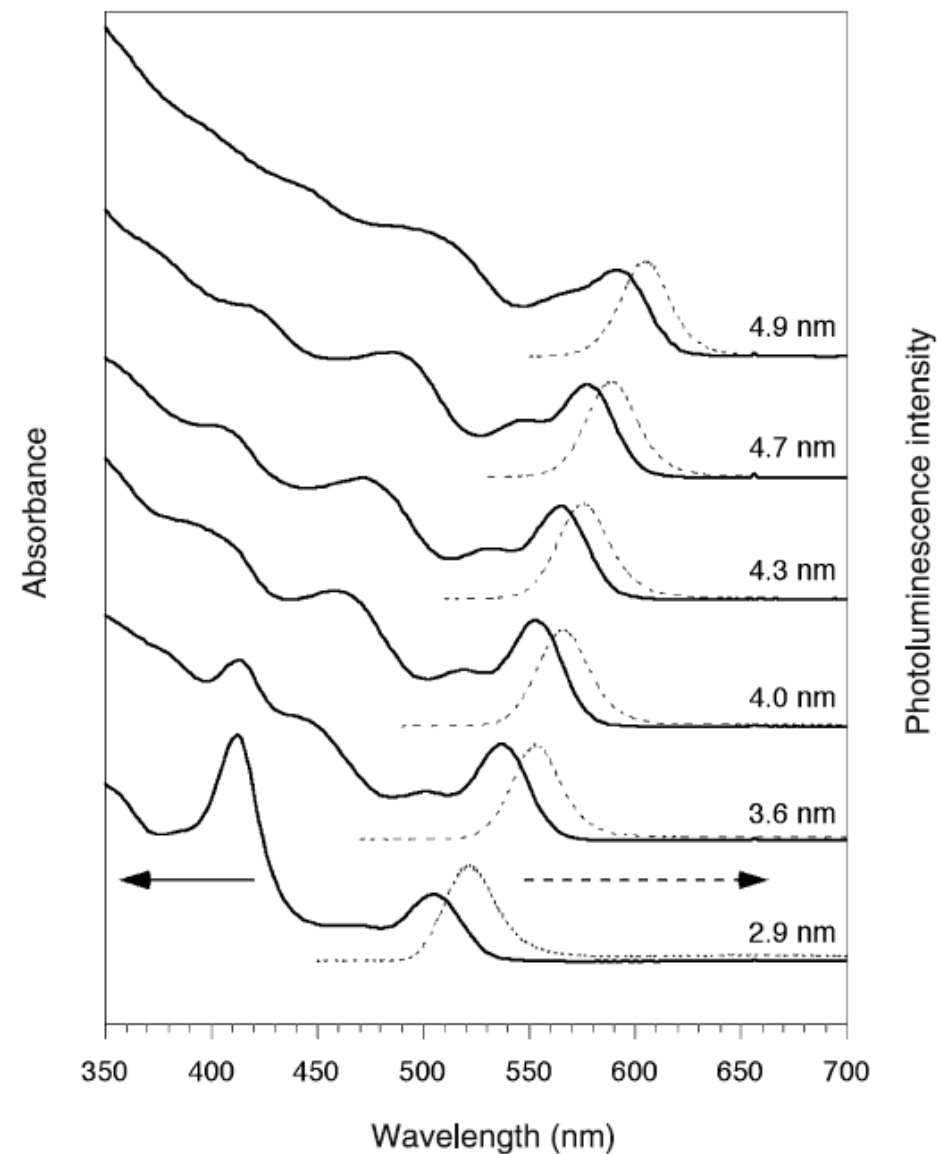
The splitting between the lowest bright and dark exciton fine structure states is analogous to the singlet-triplet splitting of the organic materials when crystal field splitting is negligible compared with the electron-hole exchange interaction.

Bright-dark exciton splitting for a selection of quantum dots: Si (tight-binding calculations), InP (fluorescence line narrowing, measured at 10 K), GaAs (pseudopotential calculations of rectangular nanocrystals), CdTe (fluorescence line narrowing, 10 K, of colloids in glass), AgI (fluorescence line narrowing, 2 K), InAs (fluorescence line narrowing, 10 K), and CdSe (fluorescence line narrowing, 10 K).

Stokes's shift in colloidal CdSe quantum dots



Schematic representation of the exciton states of CdSe NCs involved in absorption and emission processes



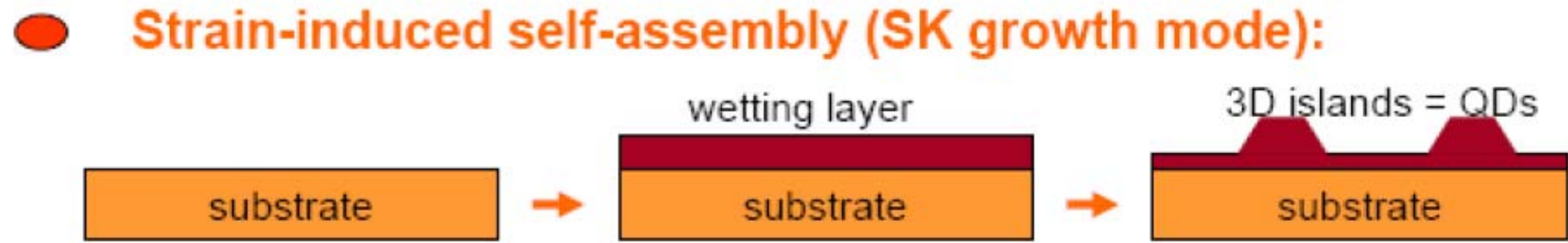
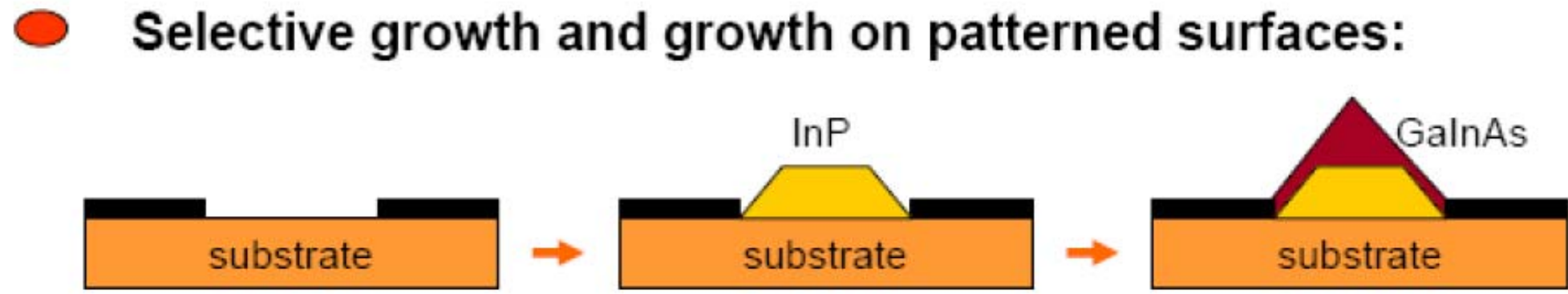
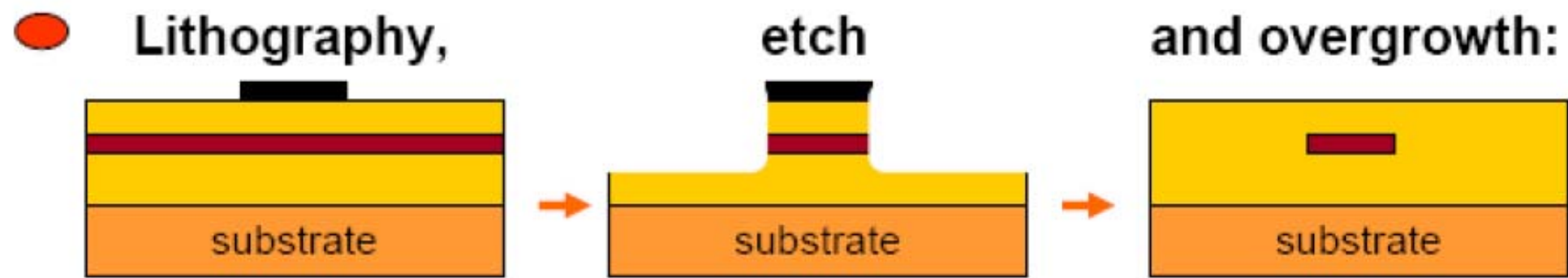
Peter Reiss, "Synthesis of semiconductor nanocrystals in organic solvents", in Andrey L. Rogach (Ed.) Semiconductor Nanocrystal Quantum Dots, Synthesis, Assembly, Spectroscopy and Applications, Springer-Verlag/Wien, 2008.

How to Make Quantum Dots?

- Top-down approaches
 - Lithography
 - Epitaxy:
 - » Patterned Growth
 - » Self-Organized Growth
- Bottom-up approaches
 - Colloidal synthesis



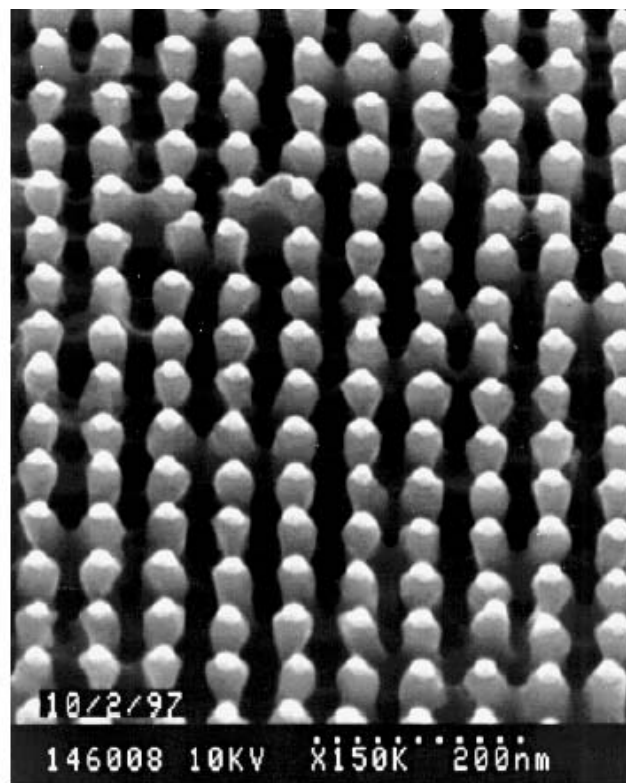
Top-down approaches



From lecture note of Prof. Sebastian Lourduoss (KTH)

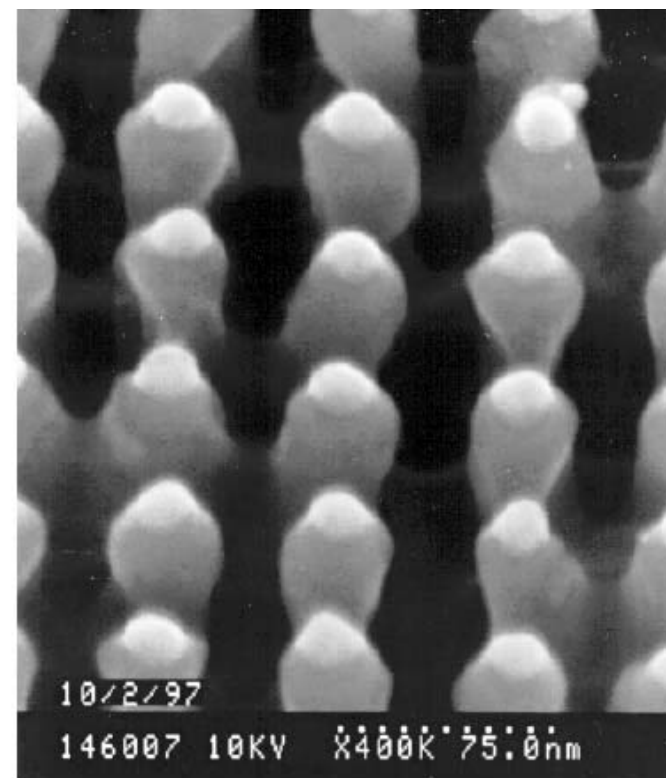


Etched Quantum Dots By E-Beam Lithography



- E-beam lithography used for Au-liftoff etch mask
- Mask size = 15-22 nm

- Etched dots have poor optical quality
- Dot density is low
- Device applications require regrowth



- $\text{SiCl}_4/\text{SiF}_4$ RIE etch
- Dot Size = 15-25 nm
- Dot Density = $3 \times 10^{10} \text{ cm}^{-2}$

Courtesy: P. Bhattacharya,
University of Michigan

From lecture note of Prof. Sebastian Lourdudoss (KTH)

Epitaxy: Patterned Growth

- Growth on patterned substrates
 - Grow QDs in pyramid-shaped recesses
 - Recesses formed by selective ion etching
 - Disadvantage: density of QDs limited by mask pattern

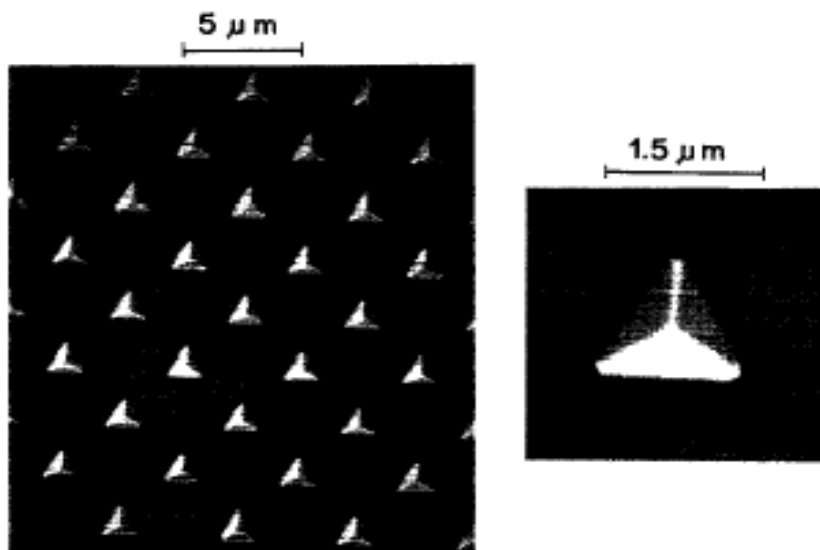
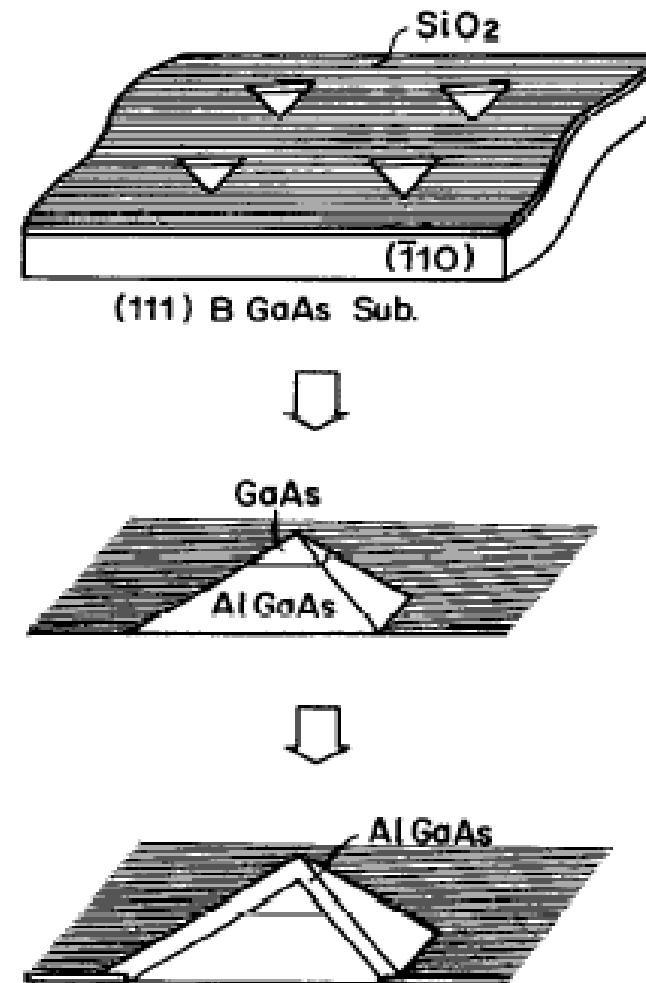


FIG. 3. Schematic view and SEM image of GaAs tetrahedral structure.

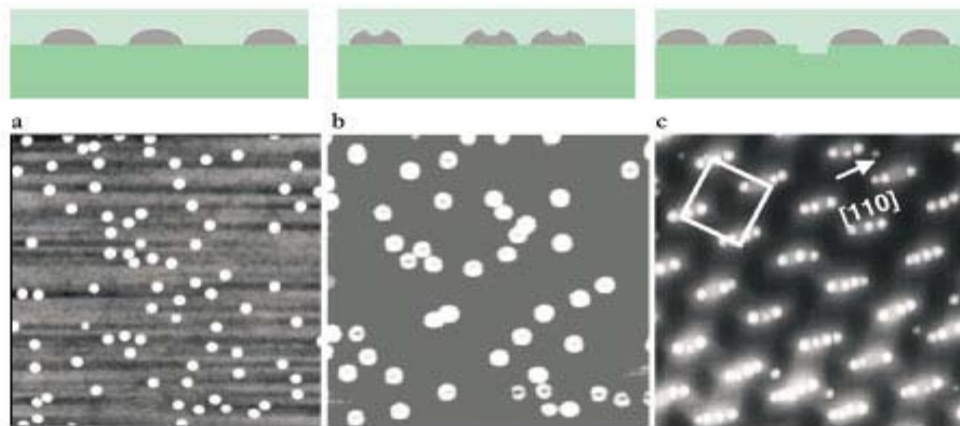


T. Fukui et al. GaAs tetrahedral quantum dot structures fabricated using selective area metal organic chemical vapor deposition. Appl. Phys. Lett. 58, 2018 (1991)

From lecture note of Prof. Joyce Poon (Caltech); <http://www.osun.org/quantum-dot-ppt.html>

Epitaxy: Self-Organized Growth

- Self-organized QDs through epitaxial growth strains
 - Stranski-Krastanov growth mode (use MBE, MOCVD)
 - Islands formed on wetting layer due to lattice mismatch (size ~ 10 s nm)
 - Disadvantage: size and shape fluctuations, ordering
 - Control island initiation
 - Induce local strain, grow on dislocation, vary growth conditions, combine with patterning



- AFM images of islands epitaxially grown on GaAs substrate.
- (a) InAs islands randomly nucleate.
 - (b) Random distribution of $\text{In}_x\text{Ga}_{1-x}\text{As}$ ring-shaped islands.
 - (c) A 2D lattice of InAs islands on a GaAs substrate.

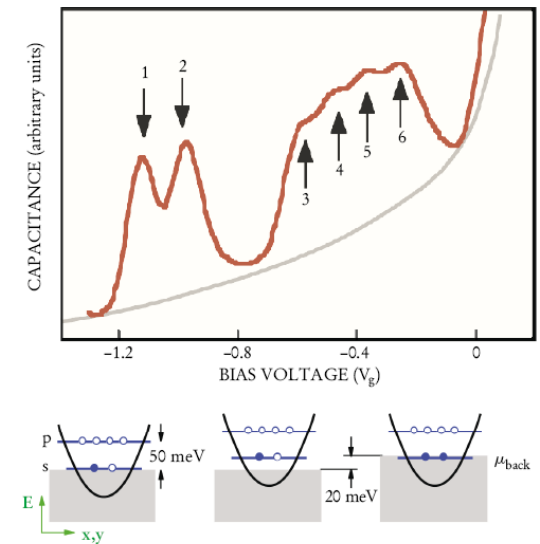
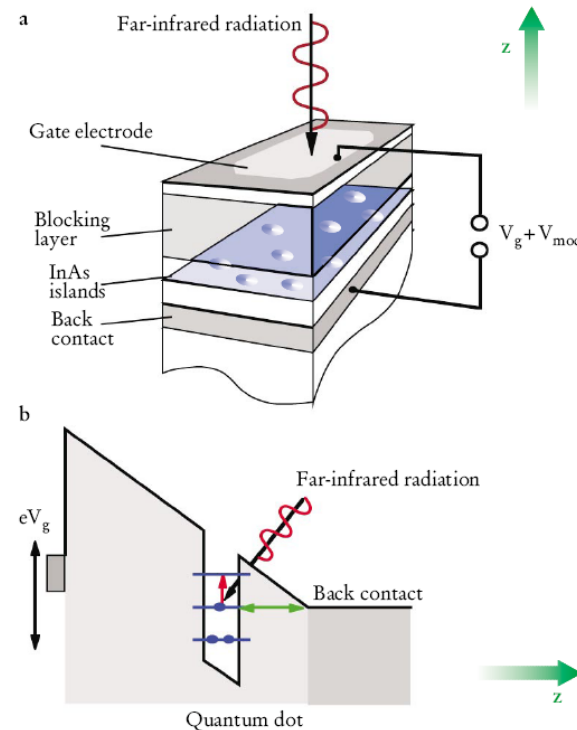


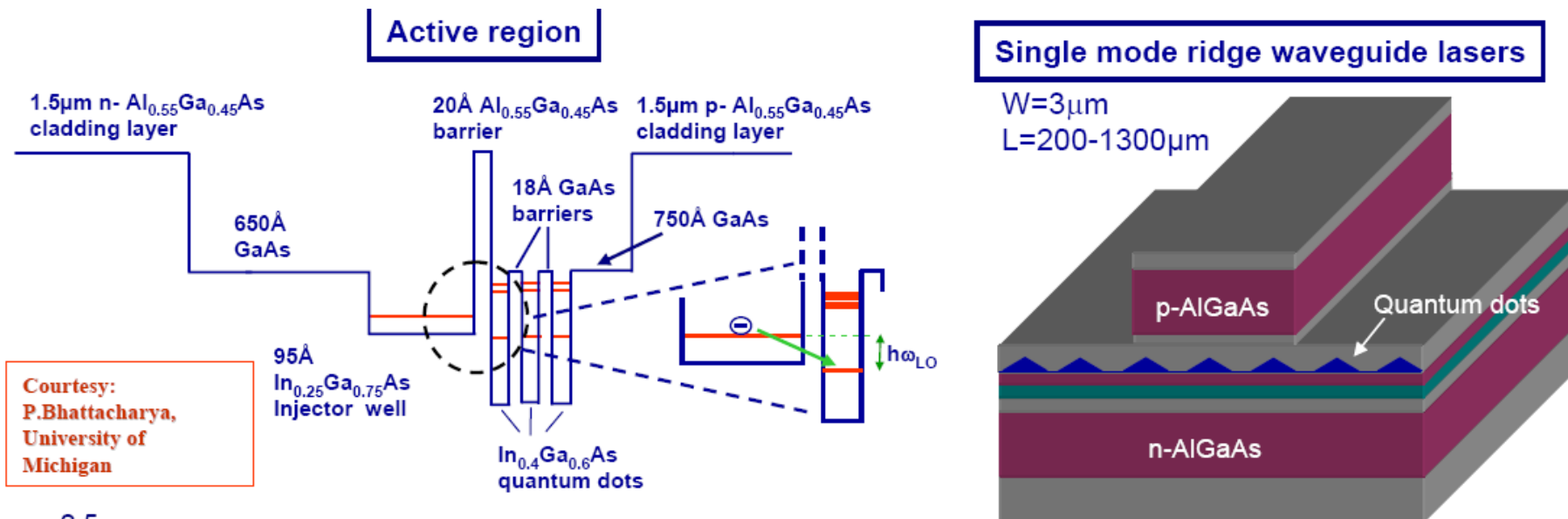
FIGURE 3. CAPACITANCE SPECTROSCOPY reveals quantum-dot electron occupancy and ground-state energies in the field-effect device shown in figure 2. Above, measured capacitance is plotted as a function of bias voltage V_g . Numbered arrows indicate the peaks that occur when an additional electron enters the dot. Below, the schematic band diagrams show the changes in the effective confining potential (black curve) and in the lowest energy levels (connected blue circles, filled in for occupied levels) as electrons are added to the quantum dot. The Fermi level μ_{back} of the back gate, which is proportional to the bias voltage, is at the top of the dark shading in the diagrams.

P. Petroff, A. Lorke, and A. Imamoglu. Epitaxially self-assembled quantum dots. *Physics Today*, May 2001, p. 46.

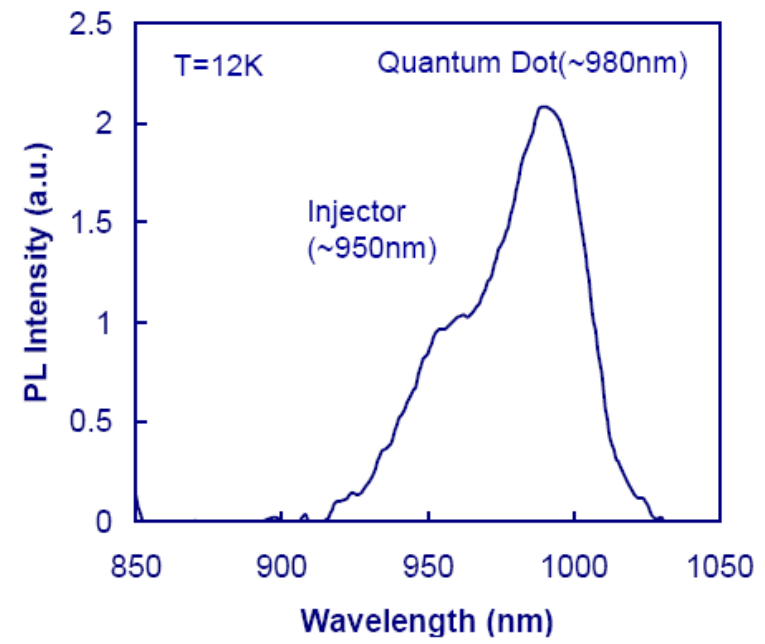
From lecture note of Prof. Joyce Poon (Caltech); <http://www.osun.org/quantum-dot-ppt.html>



Tunnel Injection QD Lasers Grown by MBE



Courtesy:
P.Bhattacharya,
University of
Michigan



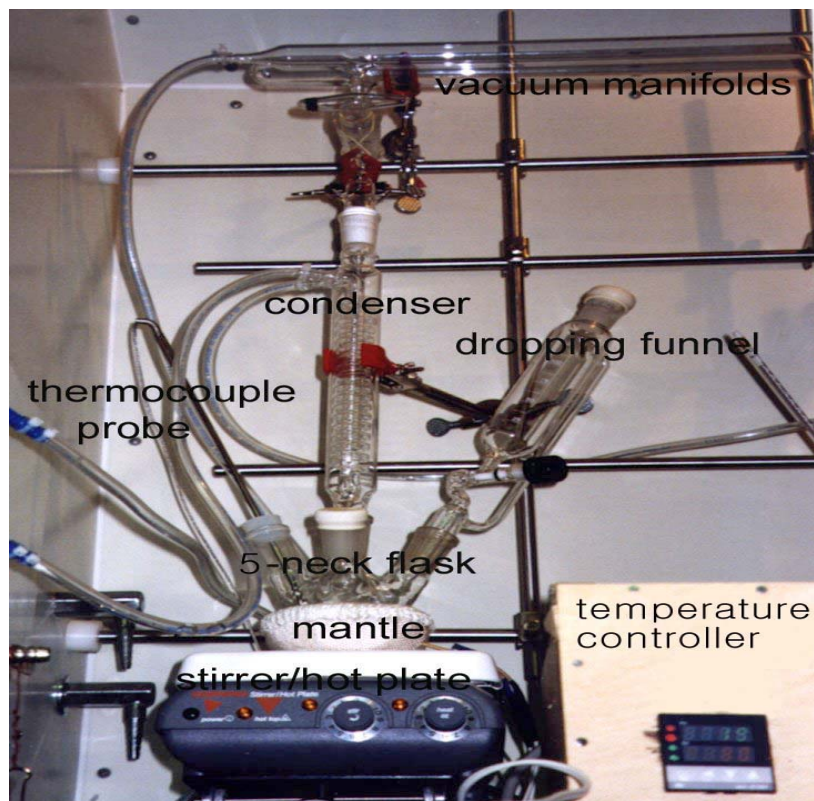
- The laser heterostructures are grown by solid source molecular beam epitaxy
- The quantum dots are grown at 530°C, the quantum well is grown at 490°C, and the rest of the structure at 630°C
- The *high strain* due to the $\text{In}_{0.25}\text{Ga}_{0.75}\text{As}$ QW limits the number of dot layers to less than 4.
- The energy separation between the quantum well injector layer ground state and quantum dot ground state is tuned by adjusting the In and Ga charge in QD

From lecture note of Prof. Sebastian Lourduoss (KTH)



Synthesis of nanomaterials through wet chemistry

Wet chemistry and self-assembly



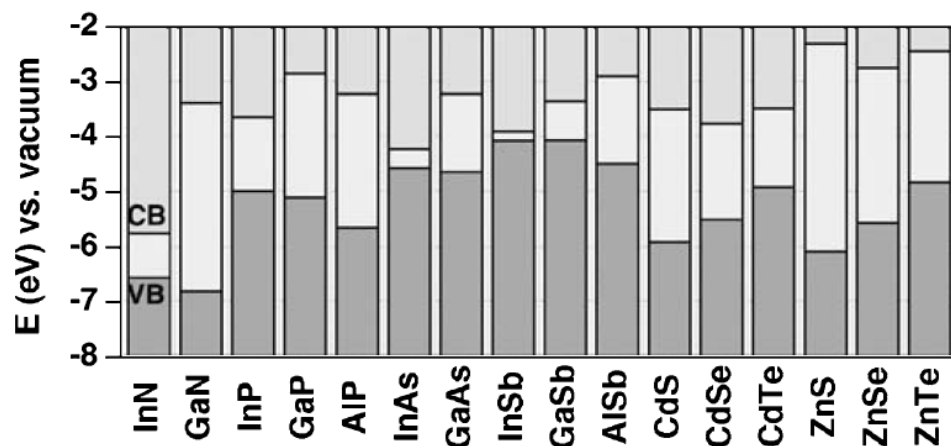
MBE/MOCVD method



- Formation of nanomaterials through wet chemistry
- Facile and cost-efficient process

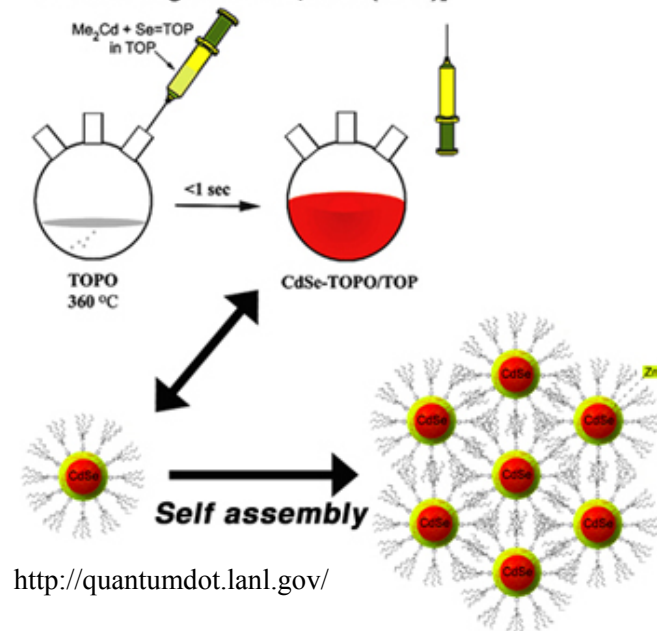
Colloidal synthesis

- Engineer reactions to precipitate quantum dots from solutions or a host material (e.g. polymer)
- In some cases, need to “cap” the surface so the dot remains chemically stable (i.e. bond other molecules on the surface)
- Can form “core-shell” structures
- Typically group II-VI materials (e.g. CdS, CdSe)
- Size variations (“size dispersion”)



Electronic energy levels of selected III-V and II-VI semiconductors using the valence band offsets from [43] (VB: valence band, CB: conduction band)

Solution-phase synthesis of semiconductor Q-dots
[per modified preps of C. Murray, et al. JACS 115, 8706 (1993) and L. Qu and X. Peng JACS 124, 2049 (2002)]



CdSe core with ZnS shell QDs

Red: bigger dots!

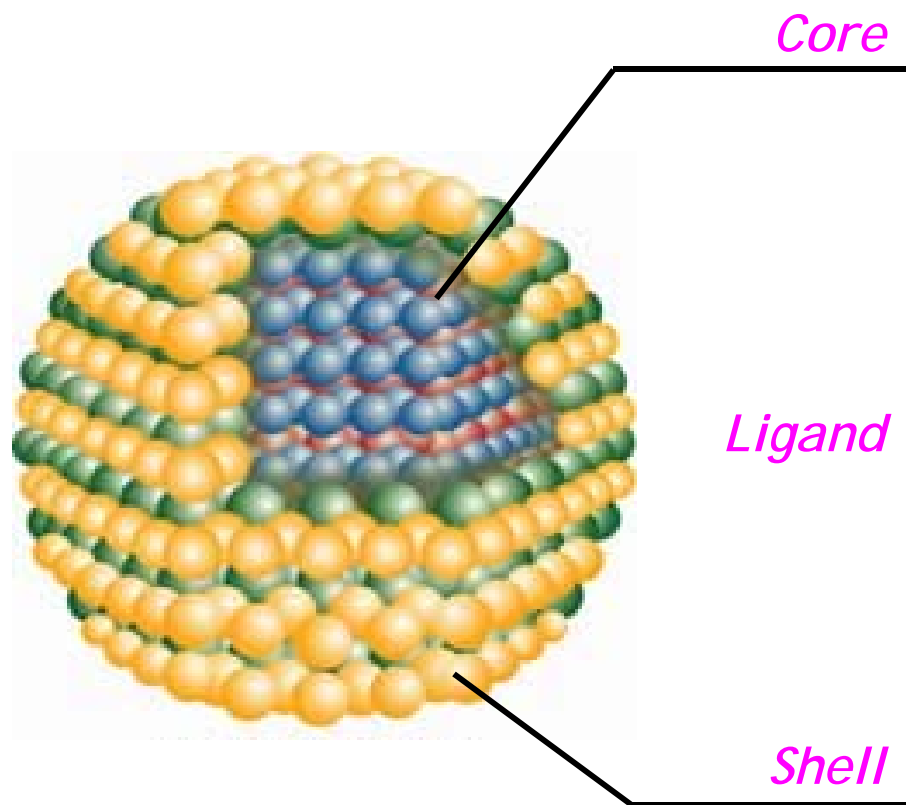
Blue: smaller dots!



Evident Technologies: http://www.evidenttech.com/products/core_shell_evidots/overview.php

M.L. Steigerwald et al., “Surface Derivatization and Isolation of Semiconductor Cluster Molecules,” *J. Am. Chem. Soc.* 110: 3046-3050 (1988).

Core@Shell Structured Colloidal Quantum Dots



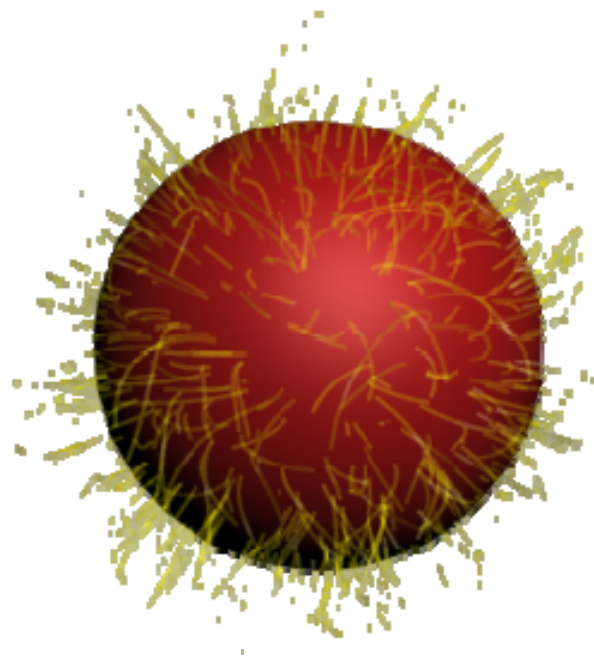
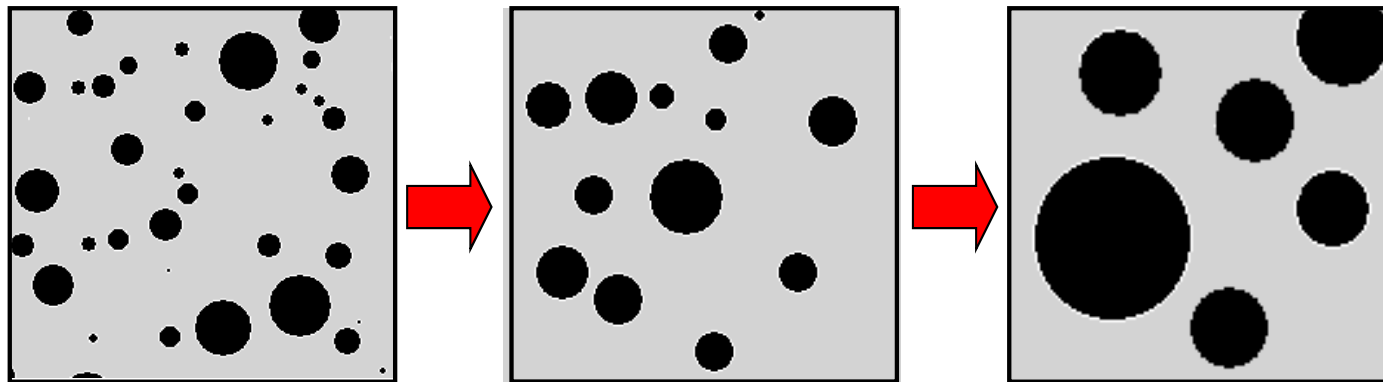
- Emission wavelength (size & composition)
- CdSe, CdTe, ZnTe, CdS (group II-VI)
- InP, InGaP (Group III-V)

- Surface stabilizer
- QD solubility
- COOH, NH₂, P, PO, PO₃

- Surface passivation (i.e. dangling bond)
- Protection layer
- ZnSe, ZnS (group II-VI)
- GaP (Group III-V)

Surface passivation of QDs

QD aggregation



Ligand

- Surface stabilizer
- QD solubility
- COOH, NH₂, P, PO, PO₃

TOPO(triethylphosphine oxide)



Chemical synthesis of semiconductor nanocrystals

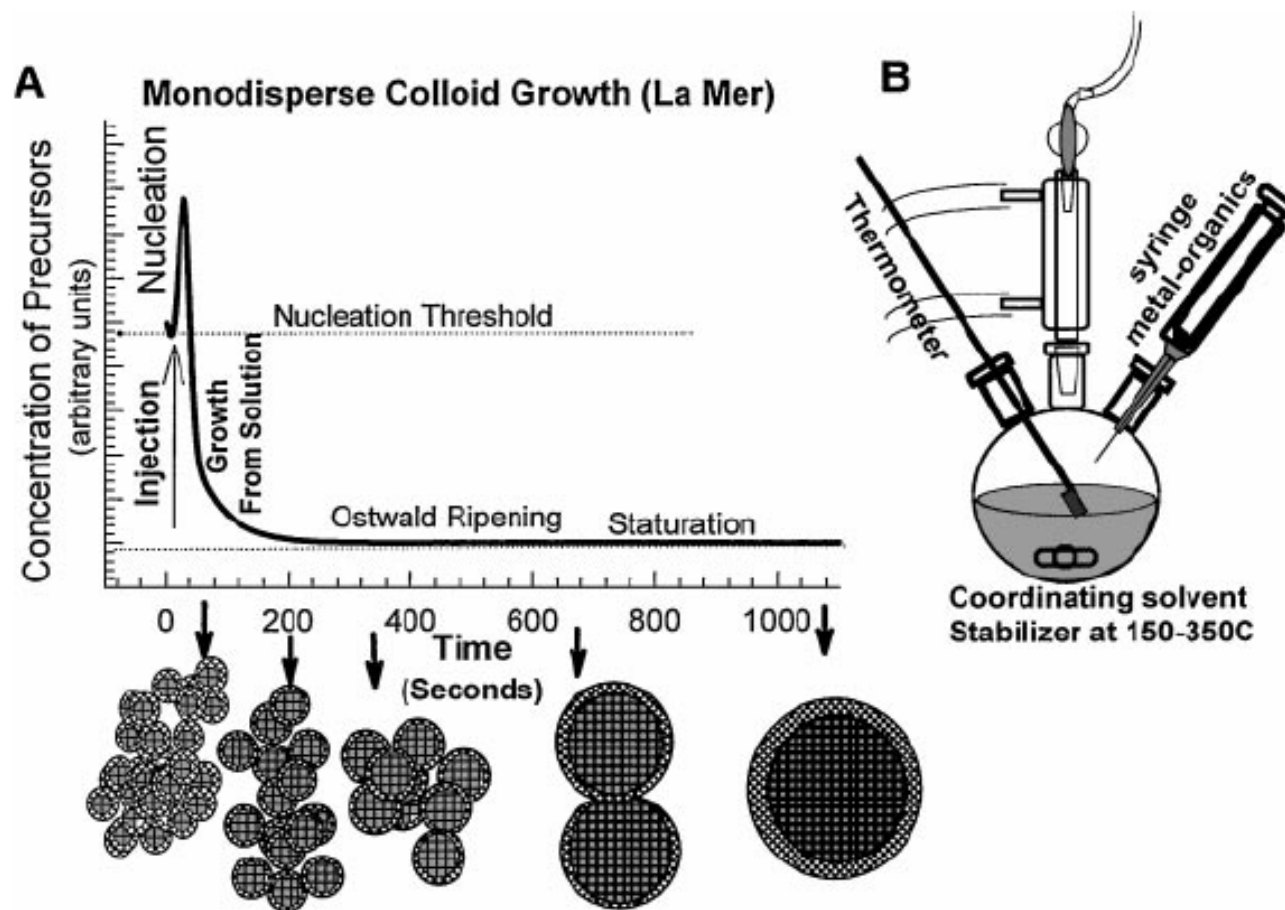
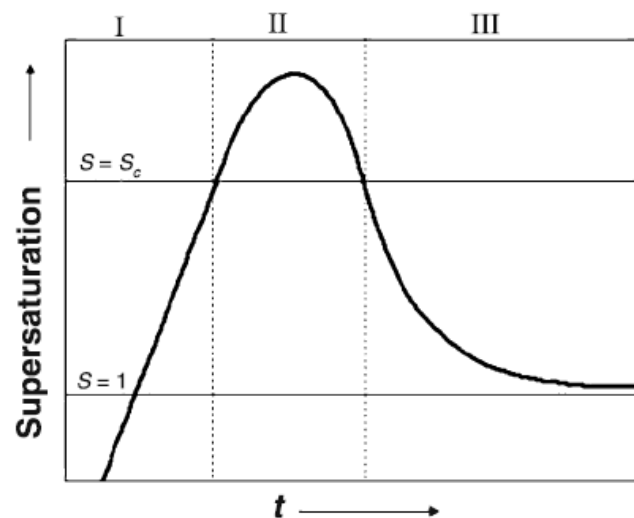


Figure 1 (A) Cartoon depicting the stages of nucleation and growth for the preparation of monodisperse NCs in the framework of the La Mer model. As NCs grow with time, a size series of NCs may be isolated by periodically removing aliquots from the reaction vessel. (B) Representation of the simple synthetic apparatus employed in the preparation of monodisperse NC samples.

C. B. Murray, C. R. Kagan, M. G. Bawendi, *Ann. Rev. Mater. Sci.* **30**, 545 (2000)

La Mer plot



LaMer plot depicting the degree of supersaturation as a function of reaction time

- Stage I:** Initially the concentration of monomers, i.e. the minimum subunits of the crystal, constantly increases by addition from exterior or by in situ generation within the reaction medium. In stage I no nucleation occurs even in supersaturated solution ($S > 1$), due to the extremely high energy barrier for spontaneous homogeneous nucleation.
- Stage II:** The energy barrier for spontaneous homogeneous nucleation is overcome for a yet higher degree of supersaturation ($S > S_c$), where nucleation and formation of stable nuclei take place. As the rate of monomer consumption induced by the nucleation and growth processes exceeds the rate of monomer supply, the monomer concentration and hence the supersaturation decreases below S_c , the level at which the nucleation rate becomes zero.

3. **Stage III:** The particle growth continues under further monomer consumption as long as the system is in the supersaturated regime.

- Experimentally, the separation of nucleation and growth can be achieved by
 - **hot-injection method:** rapid injection of the reagents into the hot solvent, which raises the precursor concentration in the reaction flask above the nucleation threshold. The hot-injection leads to an instantaneous nucleation, which is quickly quenched by the fast cooling of the reaction mixture (the solution to be injected is at room temperature) and by the decreased supersaturation after the nucleation burst.
 - **heating-up method:** the *in situ* formation of reactive species upon supply of thermal energy. This method is widely used in the synthesis of metallic nanoparticles, but recently an increasing number of examples of semiconductor NCs prepared by this approach can be found.
- Crystal growth from solution is in many cases followed by an **Ostwald ripening** process. The smallest particles dissolve because of their high surface energy and subsequently the dissolved matters redeposit onto the bigger ones. Thereby the total number of NCs decreases, whereas their mean size increases. Ostwald ripening can lead to reduced size dispersions of micron-sized colloids. In the case of nanometer-sized particles, however, Ostwald ripening generally yields size dispersions of the order of 15–20%, and therefore the reaction should be stopped before this stage.

Peter Reiss, "Synthesis of semiconductor nanocrystals in organic solvents", in Andrey L. Rogach (Ed.) Semiconductor Nanocrystal Quantum Dots, Synthesis, Assembly, Spectroscopy and Applications, Springer-Verlag/Wien, 2008.



Chemical synthesis of II-VI nanocrystals

Table 2. Precursors, stabilizers and solvents used in the synthesis of various II-VI semiconductor NCs

Material	Precursors and stabilizers	Solvent(s)	Method ^a	References
CdS, CdSe, CdTe	CdMe ₂ /TOP, (TMS) ₂ Se or (TMS) ₂ S or (BDMS) ₂ Te	TOPO	HI	[8]
CdSe	CdMe ₂ /TOP, TOP-Se	TOPO, HDA	HI	[33, 67]
CdSe, CdTe	CdO, TDPA, TOP-Se or TOP-Te	TOPO	HI	[58]
CdSe	CdO or Cd(ac) ₂ or CdCO ₃ , TOP-Se, TDPA or SA or LA	TOPO	HI	[59]
CdS, CdSe	CdO, S/ODE or TBP-Se/ODE, OA	ODE	HI	[60]
CdSe	Cd(st) ₂ , TOP-Se, HH or BP	HDA, octadecane	HI	[68]
CdSe	Cd(my) ₂ , Se, OA/ODE	ODE	HU	[69]
CdSe	CdO, Se/ODE, OA	ODE	HI	[70]
CdSe	CdO, Se, OA	Olive oil	HI	[71]
CdSe	Cd(st) ₂ , TBP-Se, SA, DDA	ODE	HI	[72]
CdS	Cd(ac) ₂ , S, MA	ODE	HU	[73]
CdS, ZnS	Cd(hdx) ₂ or Cd(ex) ₂ or Cd(dx) ₂ or Zn(hdx) ₂	HDA	HU	[74, 75]
CdS, ZnS	CdCl ₂ /OAm or ZnCl ₂ /OAm/ TOPO, S/OAm	OAm	HU	[76]
CdTe	CdMe ₂ , TOP-Te	DDA	HI	[77]
CdTe	CdO, TBP-Te/ODE or TOP-Te/ODE, OA	ODE	HI	[78, 79]
CdTe	CdO, TBP-Te, ODPa	ODE	HU	[69]
ZnS	Zn(st) ₂ , S/ODE	ODE, Tetracosane	HI	[80]
ZnS	ZnEt ₂ , S	HDA/ODE	HU	[81]
ZnSe	ZnEt ₂ , TOP-Se	HDA	HI	[82]
ZnSe	Zn(st) ₂ , TOP-Se	Octadecane	HI	[83]
ZnTe	Te and ZnEt ₂ in TOP	ODA, ODE	HI	[84]
HgTe	HgBr ₂ , TOP-Te	TOPO	HI	[85]
Cd _{1-x} Zn _x Se	ZnEt ₂ /TOP, CdMe ₂ /TOP	TOPO, HDA	HI	[86, 87]
Cd _{1-x} Zn _x Se	Zn(st) ₂ , Cd(st) ₂ , TOP-Se	ODE	HI	[88]
Cd _{1-x} Zn _x S	CdO, ZnO, S/ODE, OA	ODE	HI	[89]
CdSe _{1-x} Te _x	CdO, TOP-Se, TOP-Te	TOPO, HDA	HI	[90]

^a *HI* Hot-injection method; *HU* Heating-up method
CdMe₂ dimethylcadmium; *ZnEt₂* diethylzinc; *TMS* trimethylsilyl; *(BDMS)₂Te* bis(*tert*-butyldimethylsilyl) telluride; *TDPA* tetradecylphosphonic acid; *ODPA* octadecylphosphonic acid; *SA* stearic acid; *LA* lauric acid; *OA* oleic acid; *MA* myristic acid; *ac* acetate; *my* myristate; *st* stearate; *hdx* hexadecylxanthate; *ex* ethylxanthate; *dx* decylxanthate; *TOPO* trioctylphosphine oxide; *HAD* hexadecylamine; *DDA* dodecylamine; *ODA* octadecylamine; *TOP* trioctylphosphine; *TBP* tributylphosphine; *ODE* 1-octadecene; *HH* hexadecyl hexadecanoate; *BP* benzophenone

Peter Reiss, "Synthesis of semiconductor nanocrystals in organic solvents", in Andrey L. Rogach (Ed.) Semiconductor Nanocrystal Quantum Dots, Synthesis, Assembly, Spectroscopy and Applications, Springer-Verlag/Wien, 2008.

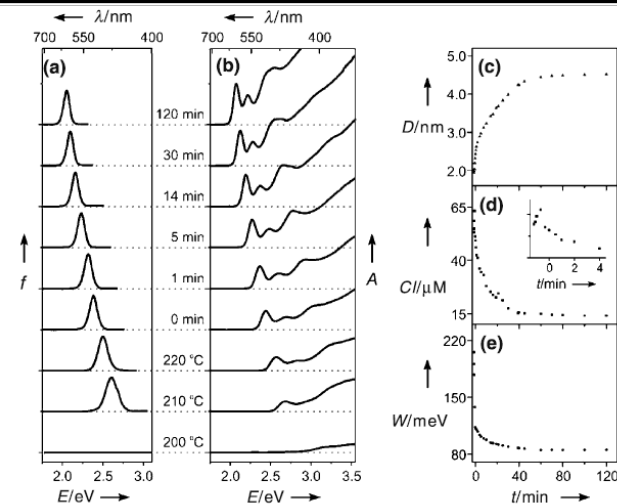


Fig. 6. Temporal evolution of **a** the fluorescence (*f*) spectrum, **b** the absorption (*A*) spectrum, **c** the diameter (*D*) of the nanocrystals, **d** (and inset) the concentration (*C*) of the nanocrystals, **e** FWHM (*W*) of the fluorescence spectrum during the phosphine-free synthesis of CdSe NCs using the heating-up method. Reproduced with permission from [69]. © 2005, Wiley-VCH Verlag GmbH & Co. KGaA

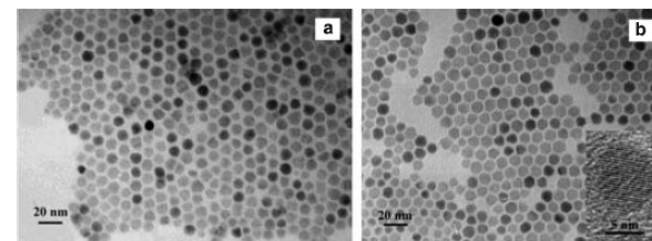


Fig. 7. TEM images of ZnS NCs synthesized via the heating-up method: **a** before size-selection process; **b** after size-selective precipitation. Inset: HRTEM image of a single ZnS NC. Reprinted with permission from I761. © 2003 American Chemical Society

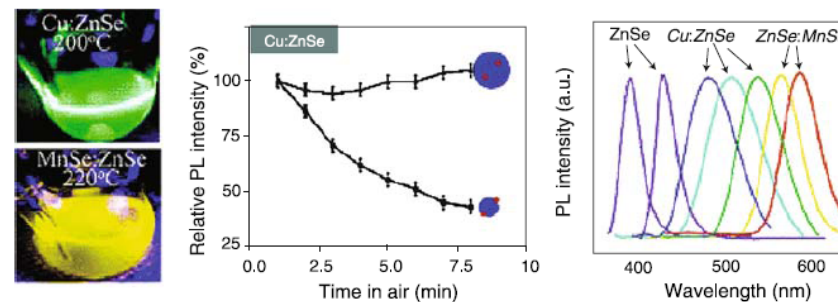


Fig. 8. Photoluminescence of Cu- and Mn-doped ZnSe NCs at high temperature (left); stability of Cu-doped ZnSe NCs in air (middle); PL spectra of ZnSe-based doped NCs. Reprinted with permission from [105]. © 2005 American Chemical Society



Chemical synthesis of III-V and IV-VI nanocrystals

Table 3. Precursors, stabilizers and solvents used in the synthesis of various III–V semiconductor NCs

Material	Precursors and stabilizers	Solvent(s)	References
InP	InCl ₃ or InCl ₃ /Na ₂ C ₂ O ₄ , P(TMS) ₃	TOPO or TOPO/TOP	[110, 111]
InP, InAs	In(ac) ₃ , P(TMS) ₃ or As(TMS) ₃ , MA	ODE	[112]
InP	InMe ₃ , P(TMS) ₃ , MA	MM or DBS,	[113]
InAs	InCl ₃ , As(TMS) ₃	TOP	[114]
GaP	[Cl ₂ GaP(SiMe ₃) ₂] ₂	TOPO/TOP	[115]
GaP	Ga(PrBu ₂) ₃	TOA, HDA	[116]
GaP	GaCl ₃ , P(TMS) ₃	TOPO	[117]
GaN, AlN, InN	[M(H ₂ NCONH ₂) ₆]Cl ₃ (M=Ga, Al, In)	TOA	[118]

TMS trimethylsilyl; *ac* acetate; *MA* myristic acid; *OA* oleic acid; *TOPO* trioctylphosphine oxide; *TOP* trioctylphosphine; *ODE* 1-octadecene; *MM* methyl myristate; *DBS* dibutyl sebacate; *TOA* trioctylamine; *HDA* hexadecylamine

Table 4. Precursors, stabilizers and solvents used in the synthesis of various IV–VI semiconductor NCs

Material	Precursors and stabilizers	Solvent	References
PbSe	Pb(ac) ₂ , OA, TOP-Se	DPE	[122, 128–132]
PbSe	Pb(chbt) ₂ , TBP-Se	TOPO	[133]
PbSe	PbO, OA, TOP-Se	ODE	[124]
PbS	PbO, OA, (TMS) ₂ S	ODE	[125]
PbS	PbCl ₂ , S/OAm	OAm	[76]
PbTe	Pb(ac) ₂ , OA, TOP-Te	DPE	[126]
PbTe	PbO, OA, TOP-Te	ODE	[127]

TMS trimethylsilyl; *ac* acetate; *chbt* cyclohexylbutyrate; *OA* oleic acid; *OAm* Oleylamine; *DPE* diphenylether

Synthesis of core/shell nanocrystals

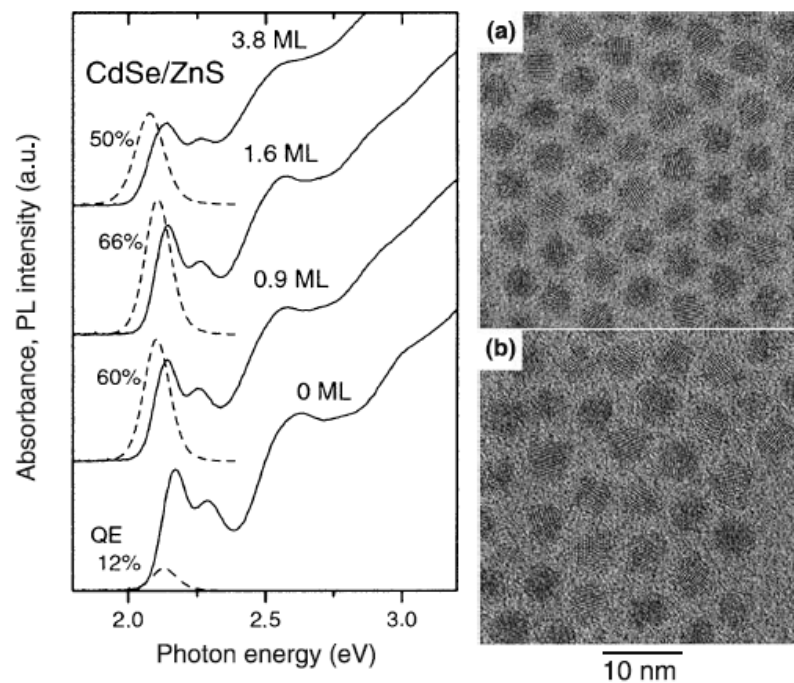


Fig. 10. Left panel: UV-vis absorption and PL spectra during the growth of a ZnS shell (ML= monolayer) on 4 nm CdSe NCs. Right panel: TEM images of 4 nm core NCs (a) and of CdSe/ZnS CS NCs (b; 1.6 ZnS ML). Reprinted with permission from [33]. © 2001, American Chemical Society

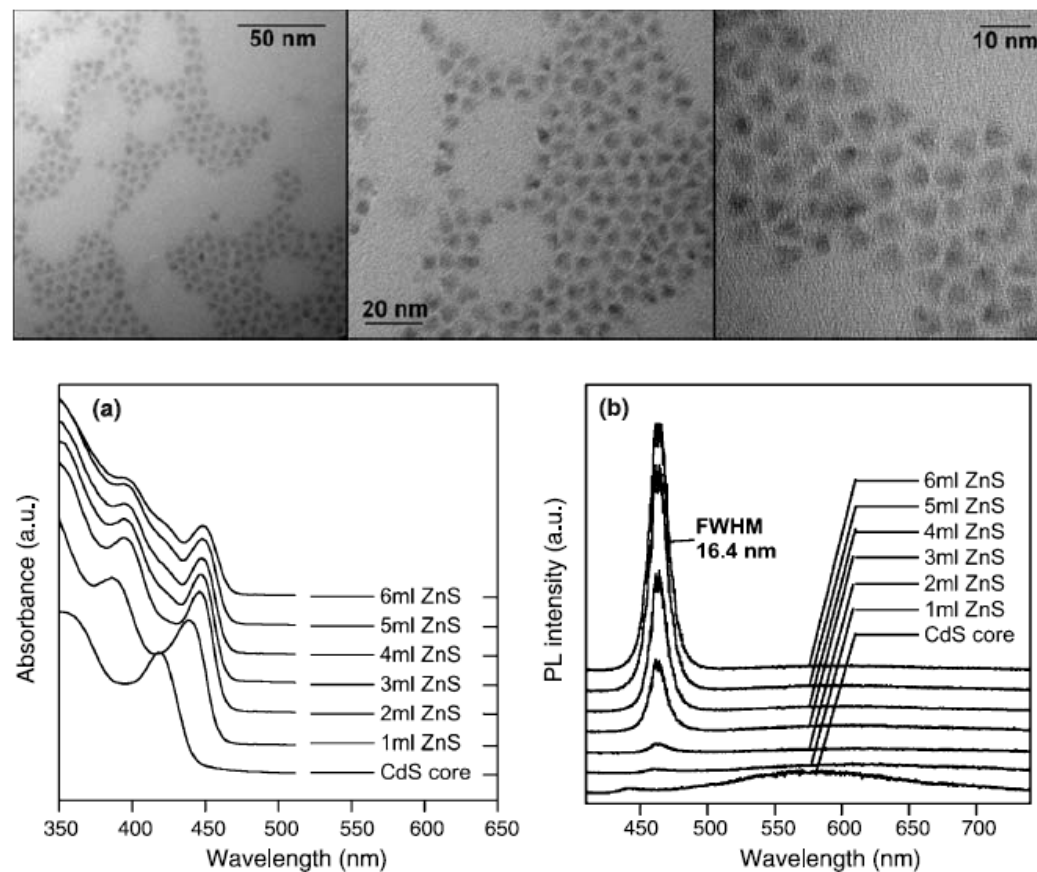
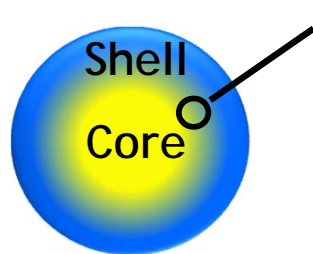


Fig. 11. Top: TEM images at different magnifications of CdS/ZnS NCs using zinc ethylxanthate as precursor for the ZnS shell growth. Bottom: **a** UV-vis absorption spectra; **b** PL spectra recorded during the addition of 6 mL of the ZnS precursor solution corresponding to the growth of a five monolayer-thick ZnS shell on 4 nm CdS core NCs [168]

Synthesis of Highly Luminescent Quantum Dots



Improved interface

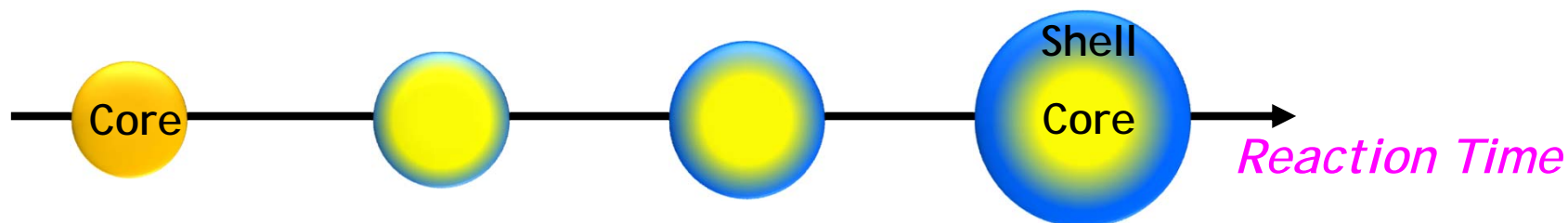
Key Issues:

- *Relieved lattice mismatch btw core and thick shell*
- *Uniform shell growth*
- *Straightforward and reproducible synthetic manner*

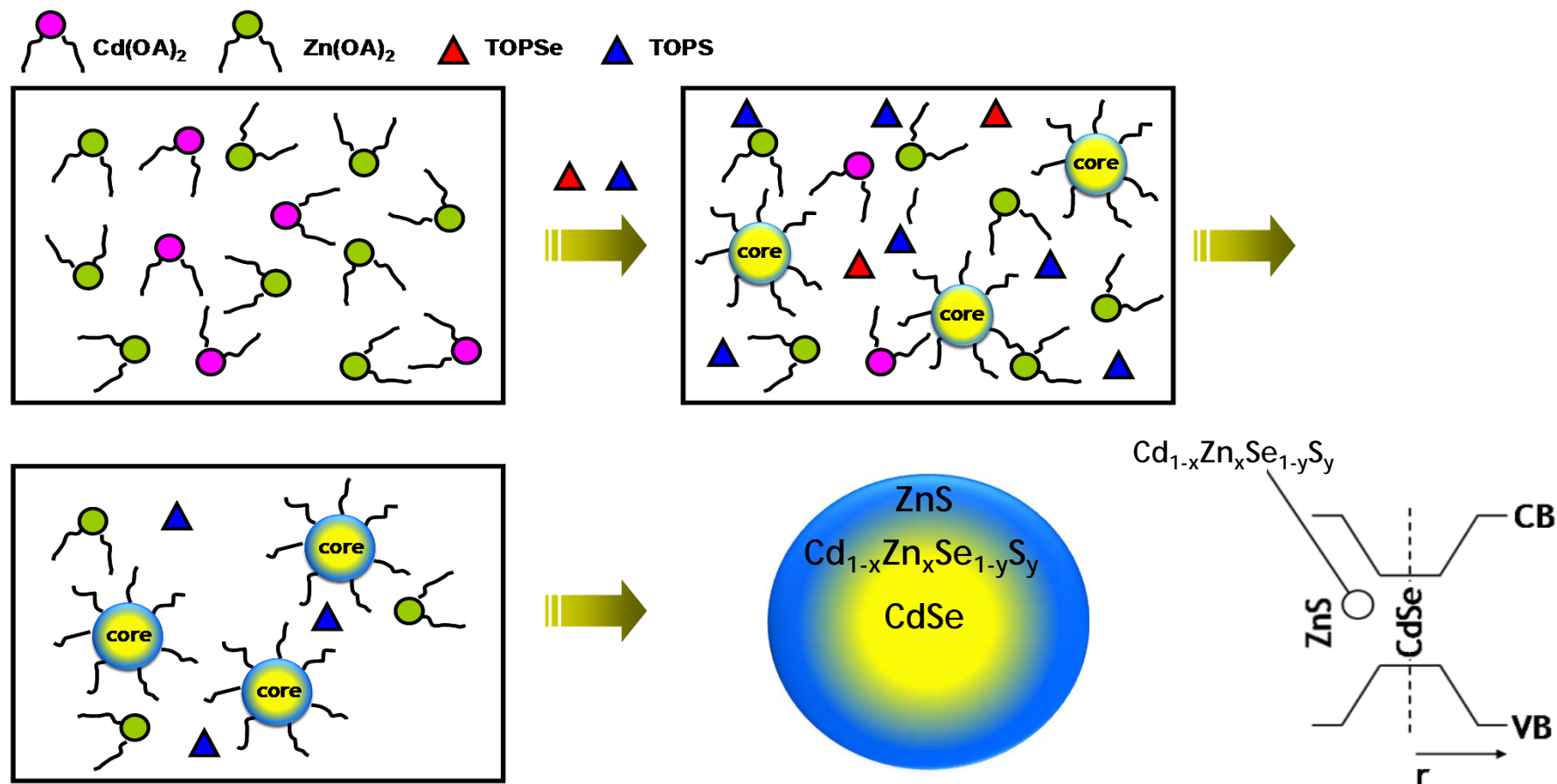
Strategy 1: Improved interface through post treatment (thermal annealing)



Strategy 2: Composition gradient shell growth



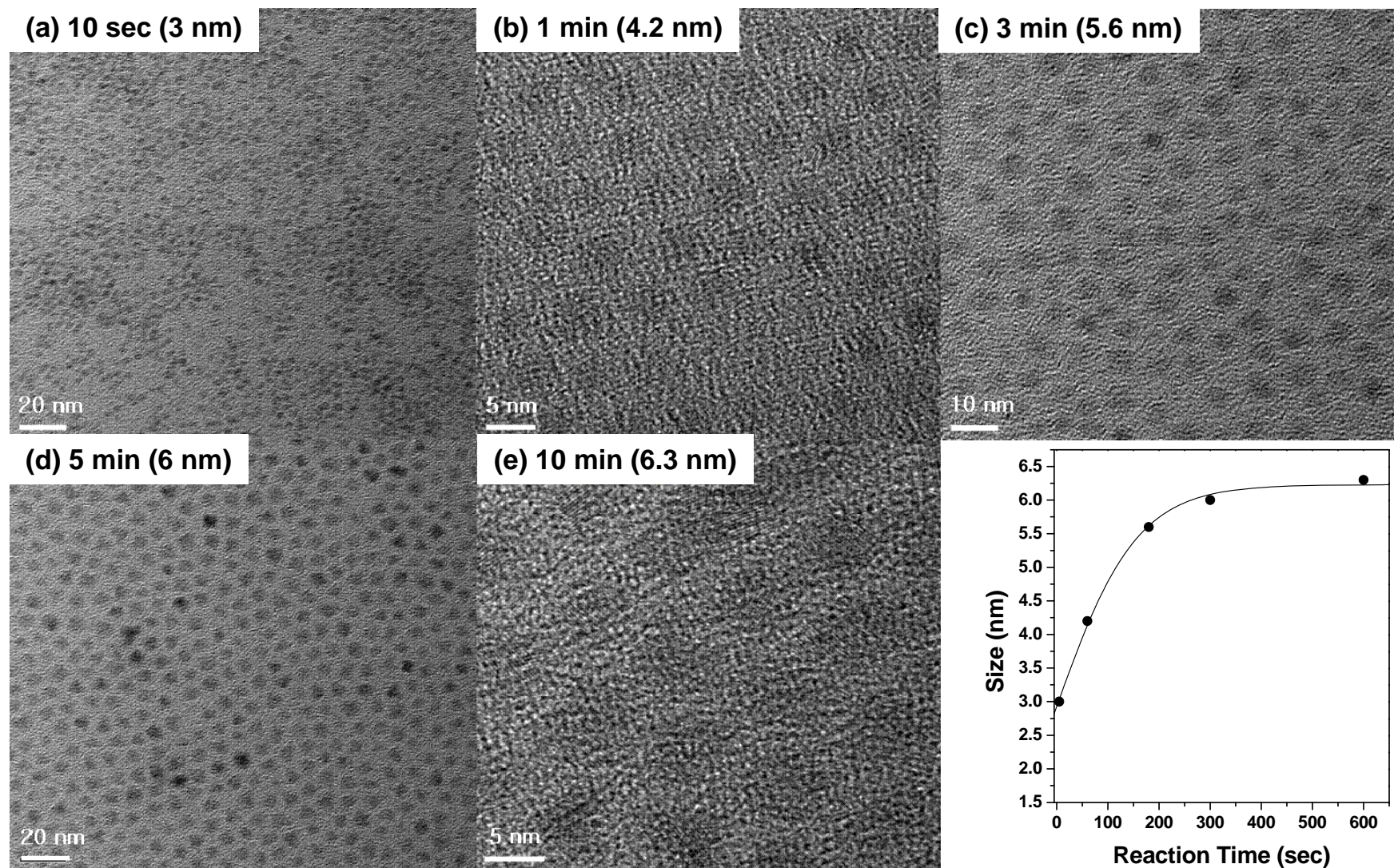
One-Pot Synthesis of Quantum Dots (Green/Red)



- *Straightforward and efficient*
- *Quantum dots with wide emission range (Green ~ Red)*
- *General method to synthesize QDs with composition gradients*
- *A gram-scale synthesis with minimum amount of surfactants*

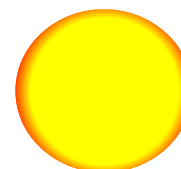
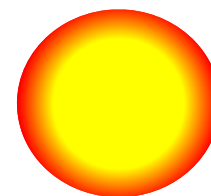
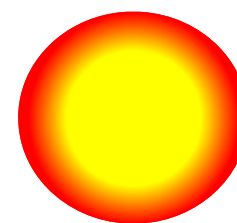
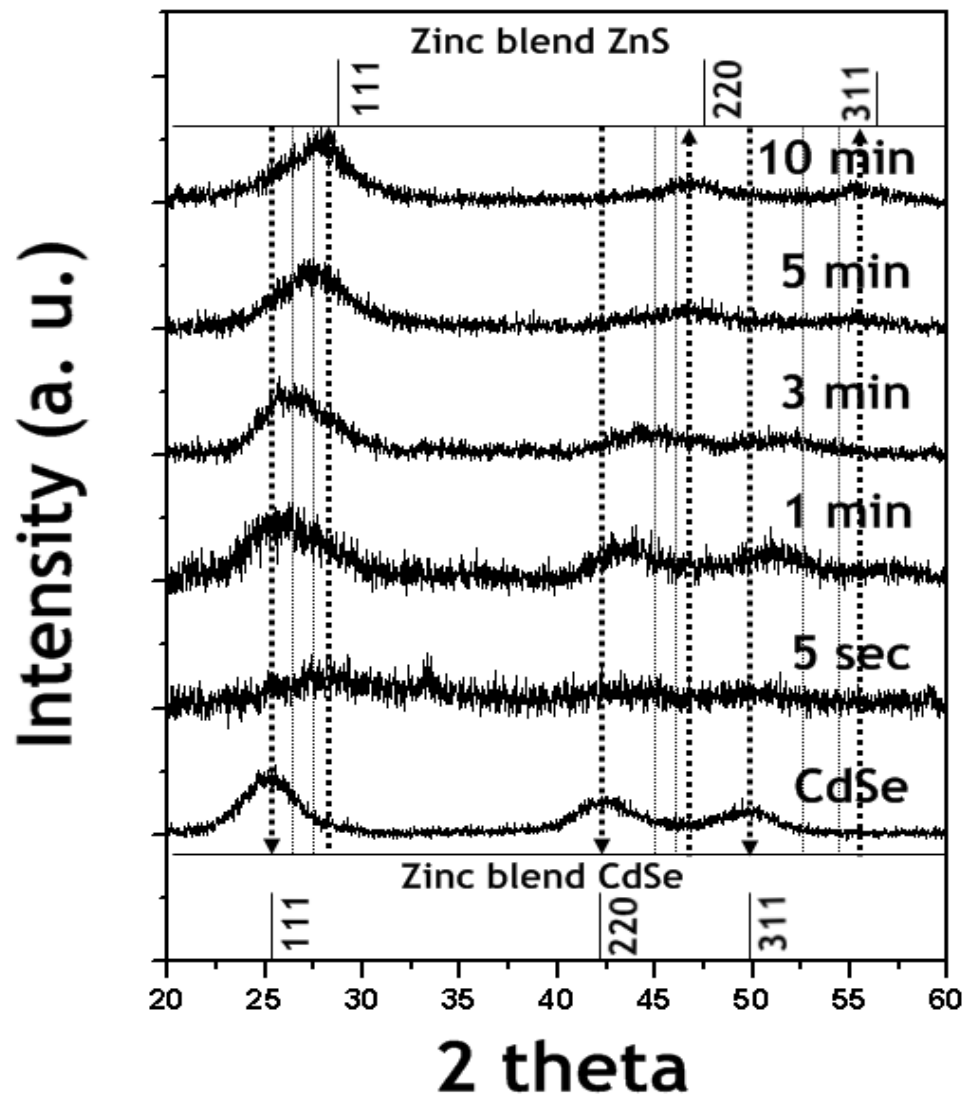
One-Pot Synthesis of Quantum Dots (Green/Red)

TEM images of QDs as a function of reaction time



Quantum dots possess spherical shape with narrow size distribution ($\sigma < 5\%$).

Composition Analysis on Quantum Dots (Green/Red)

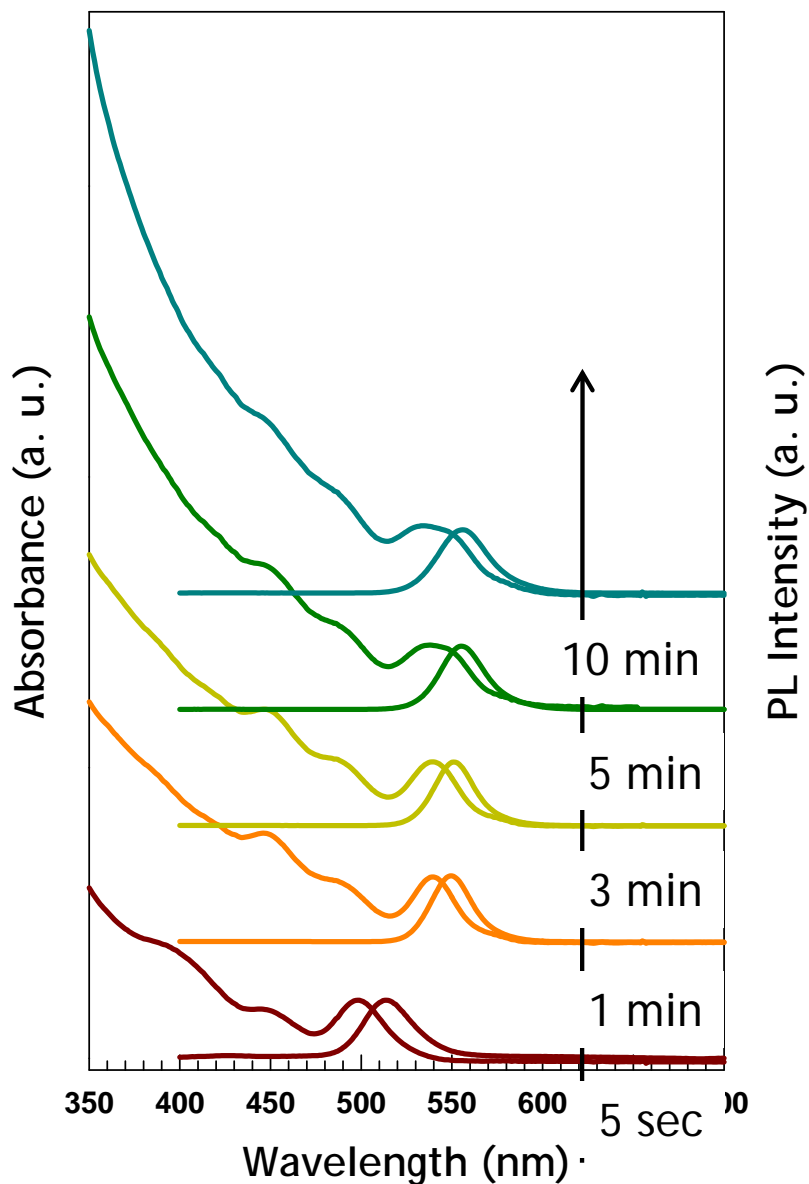


Zinc Blend CdSe@ZnS

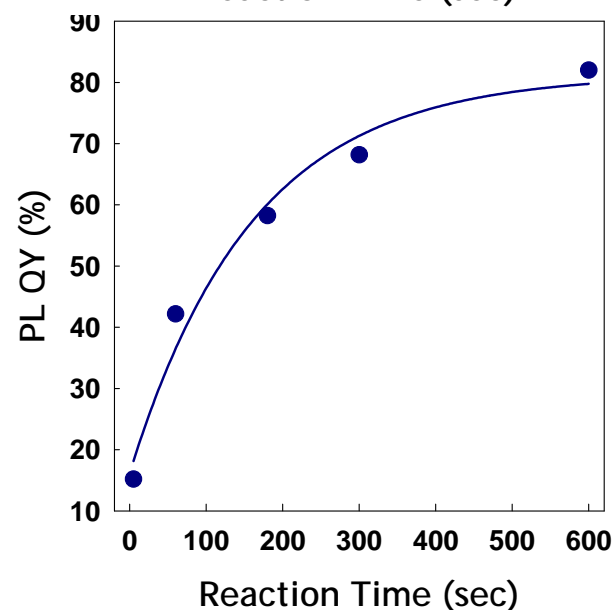
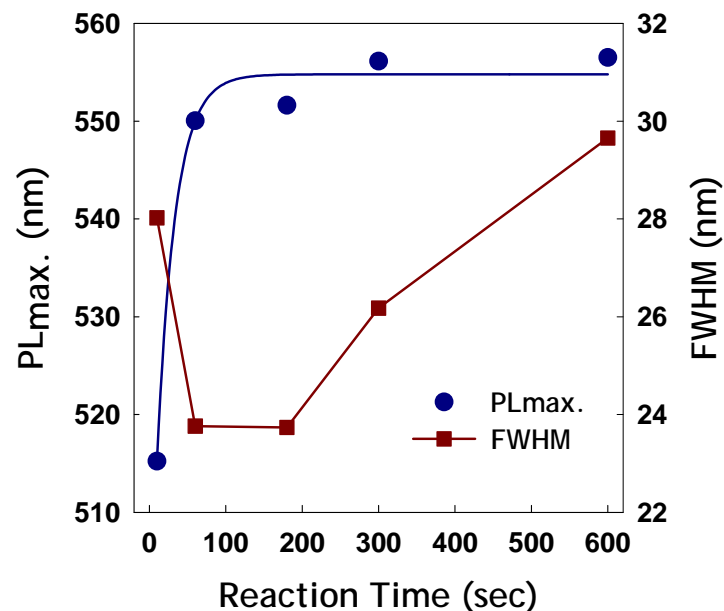


Zinc Blend CdSe

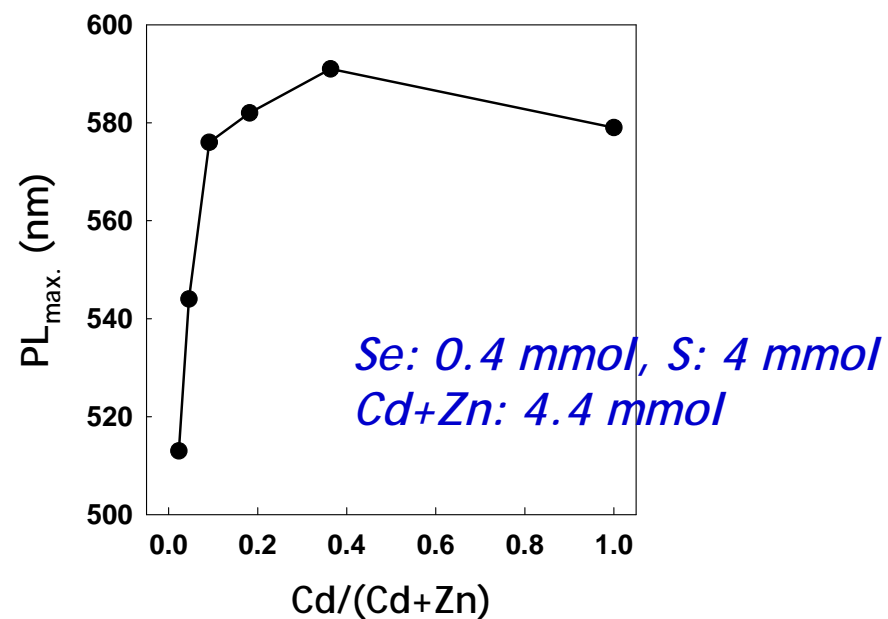
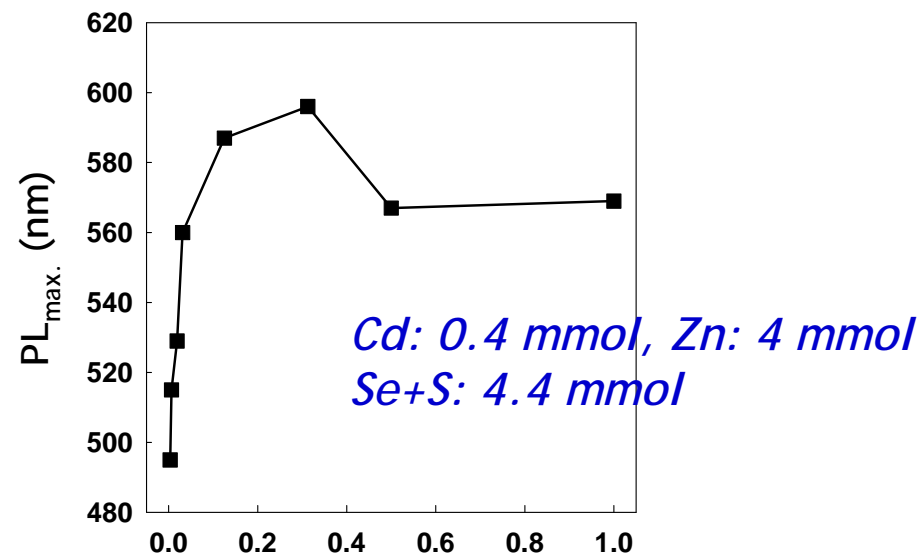
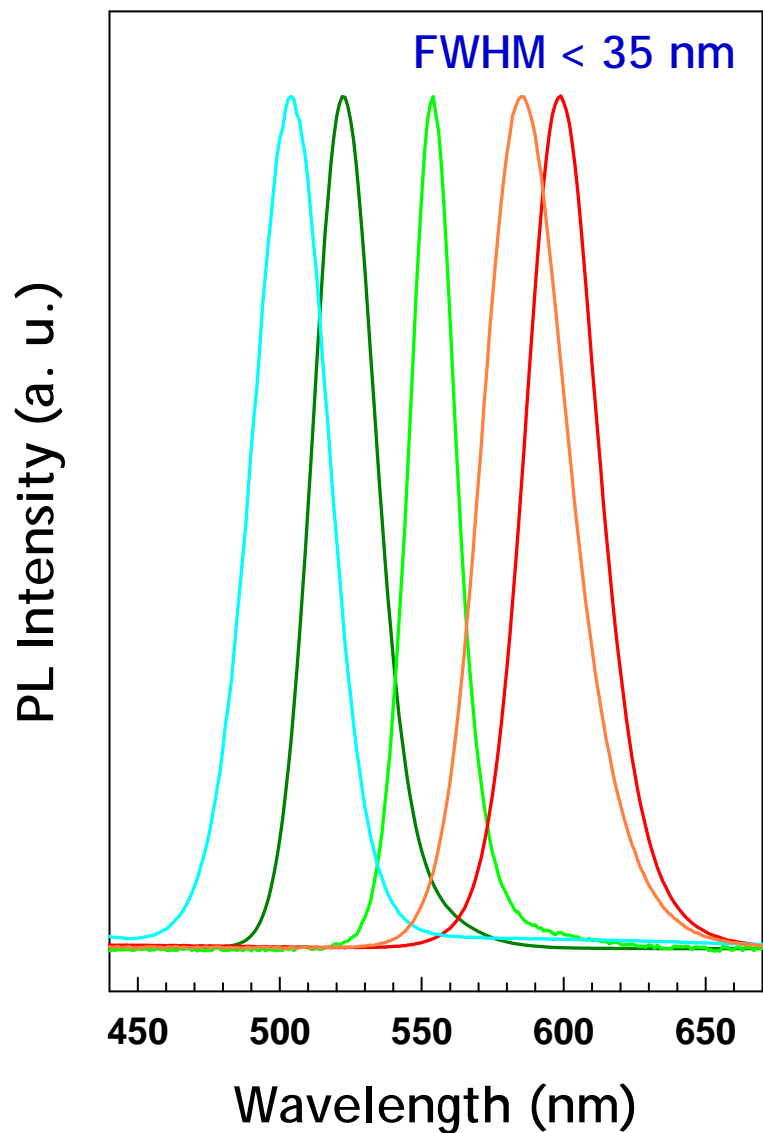
UV-Vis. & PL Spectra of Quantum Dots (Green/Red)



PL Intensity (a. u.)

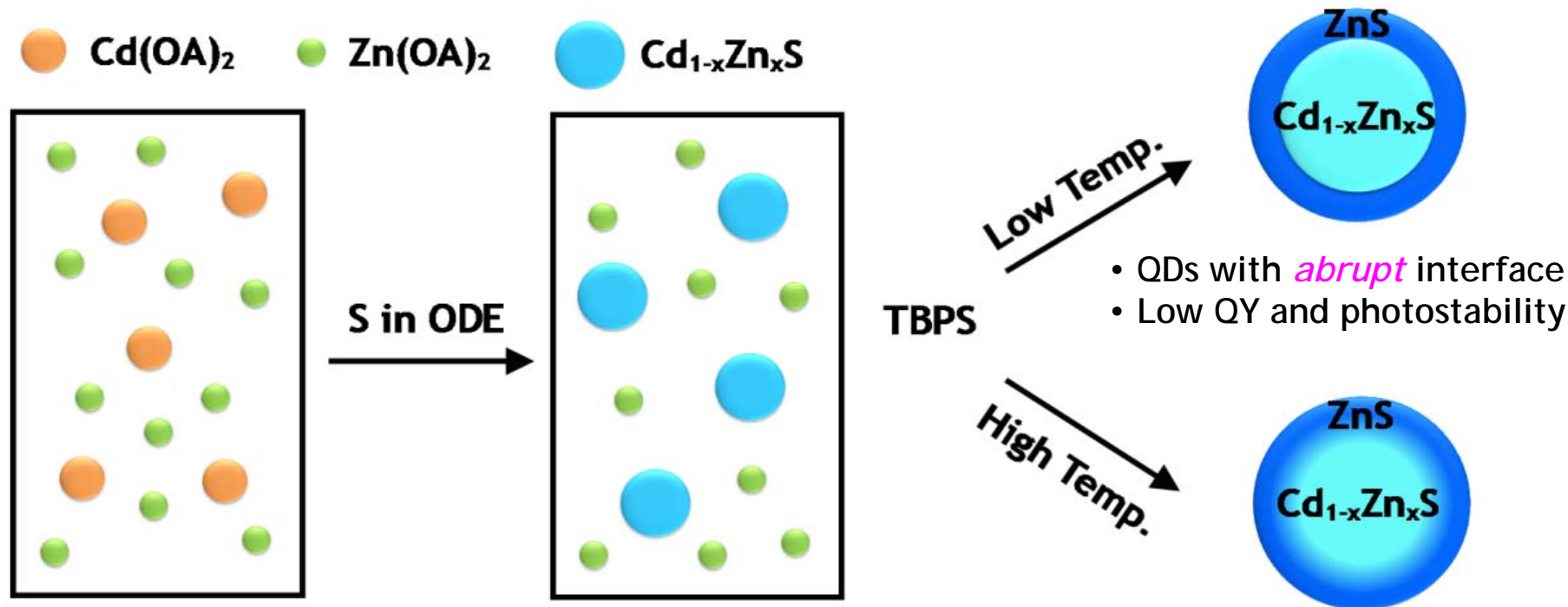


Emission Window of Quantum Dots (Green/Red)



Preparation of $\text{Cd}_{1-x}\text{Zn}_x\text{S}@Zn\text{S}$ Quantum Dots (Blue)

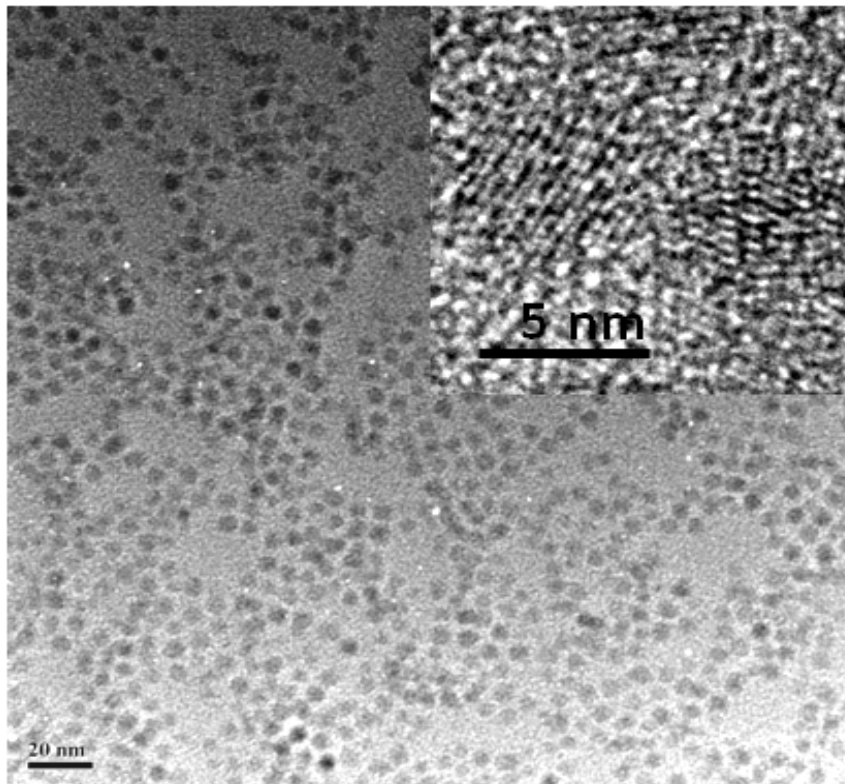
Reaction schematic for $\text{Cd}_{1-x}\text{Zn}_x\text{S}@Zn\text{S}$ quantum dots



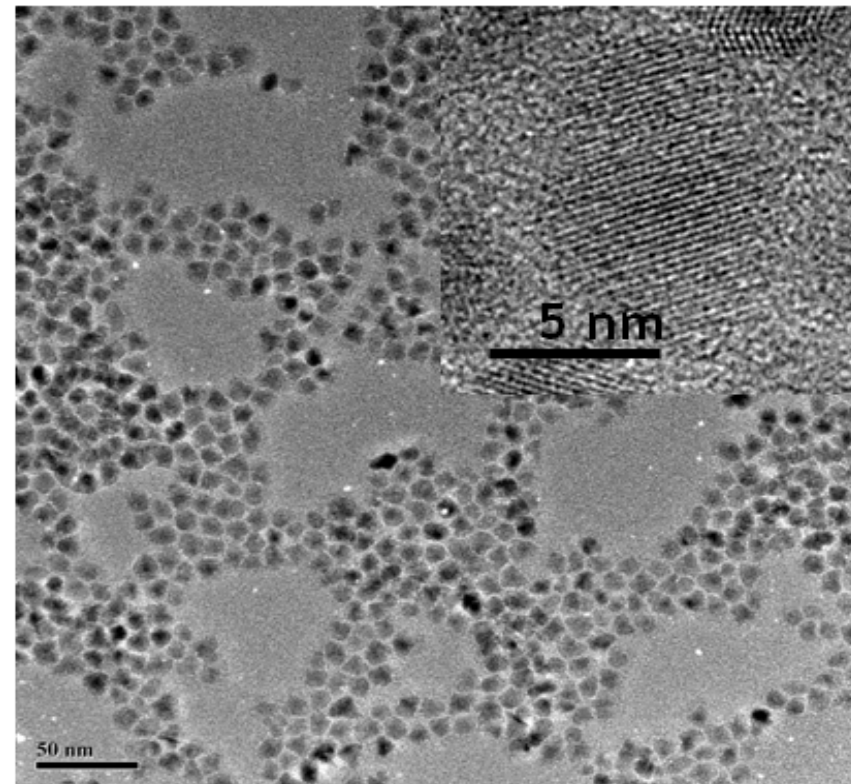
- *Straightforward and efficient (one-pot synthetic method)*
- *Quantum dots with emission range from near UV to blue*
- *General method to synthesize QDs with improved interface*
- *A gram-scale synthesis with minimum amount of surfactants*

Preparation of $\text{Cd}_{1-x}\text{Zn}_x\text{S}@Zn\text{S}$ Quantum Dots (Blue)

$\text{Cd}_{1-x}\text{Zn}_x\text{S}$ quantum dots

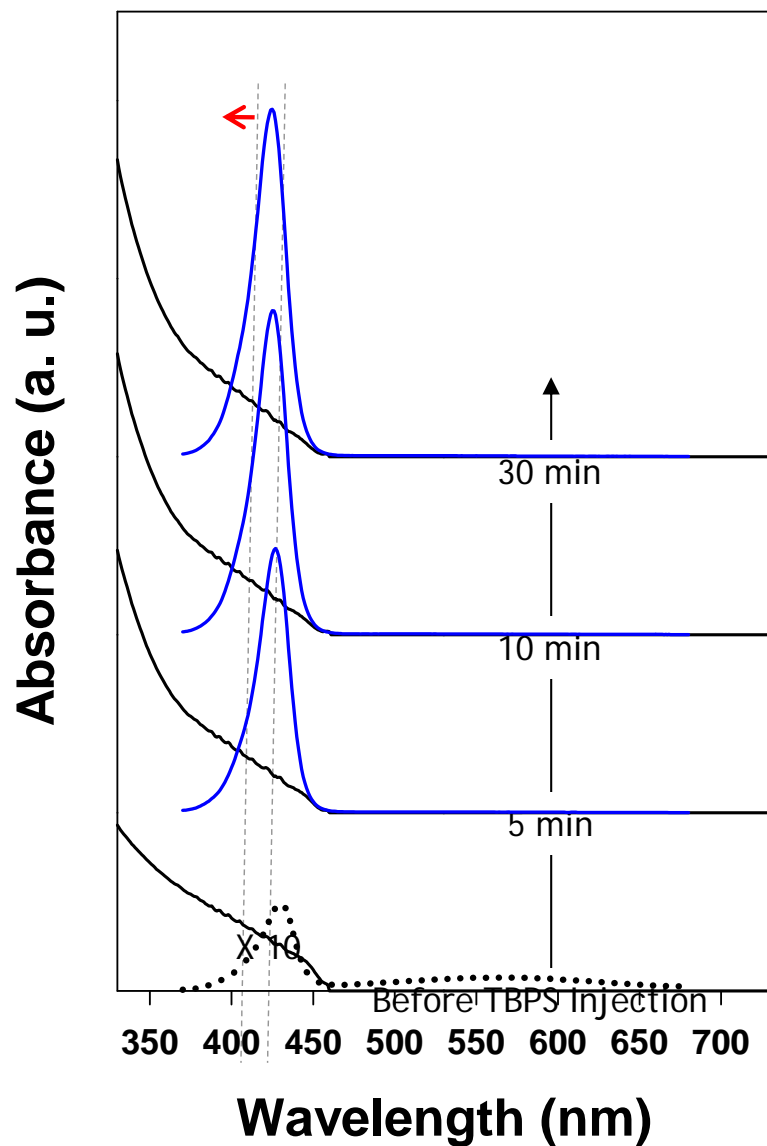


$\text{Cd}_{1-x}\text{Zn}_x\text{S}@Zn\text{S}$ quantum dots

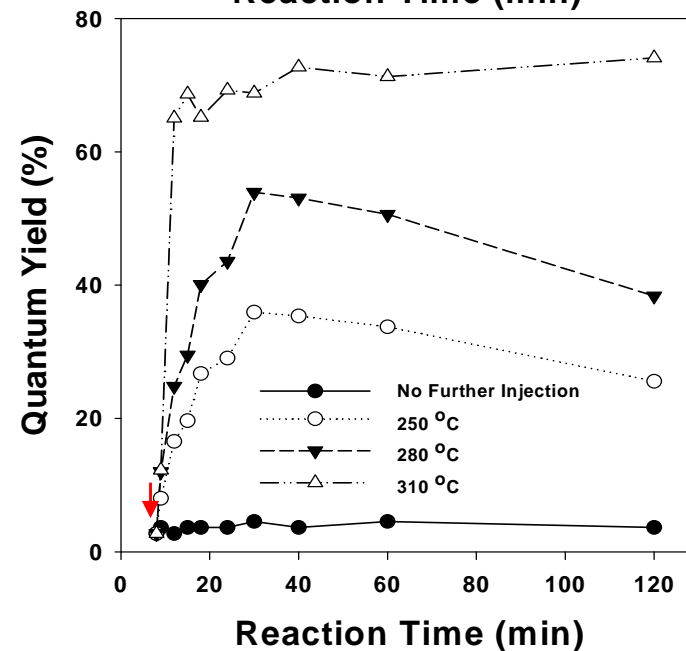
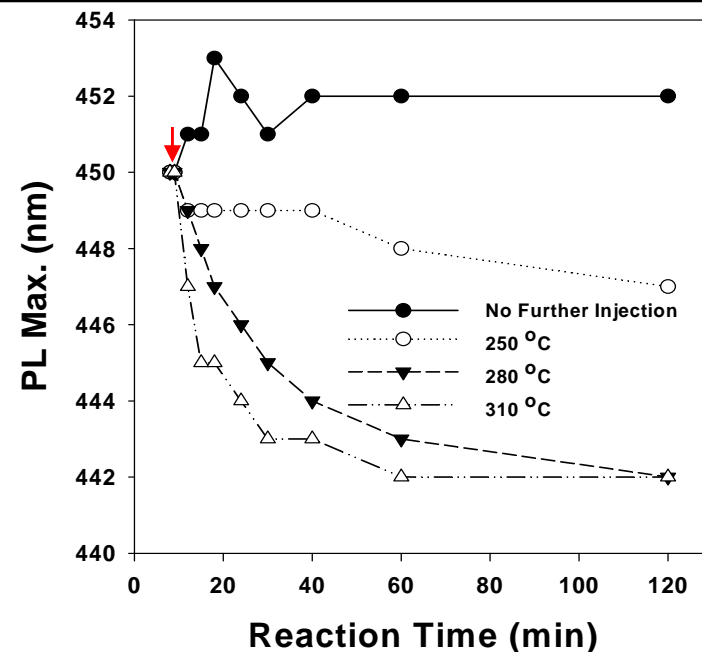


- *The size of quantum dots increase about 3 nm.*
- *Quantum dots possess spherical shape with high crystallinity.*

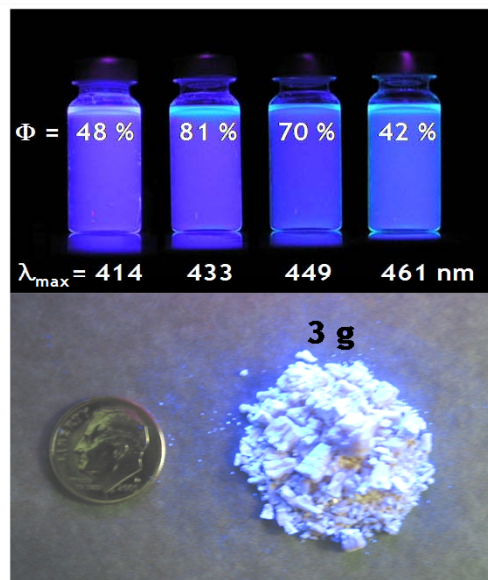
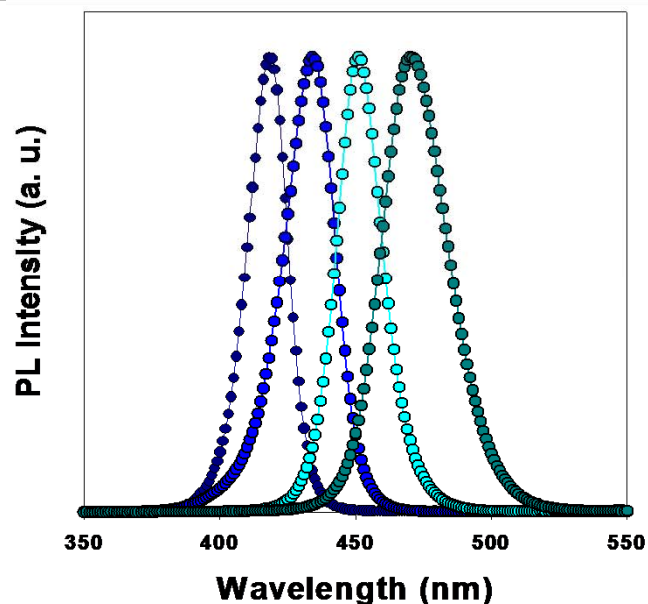
UV-Vis. & PL Spectra of $\text{Cd}_{1-x}\text{Zn}_x\text{S}@Z\text{nS}$ Quantum Dots (Blue)



PL Intensity (a. u.)



Emission Window & Scale-up Capability of Cd_{1-x}Zn_xS@ZnS QDs (Blue)



Deep Blue QDs

- From violet (410 nm) to blue (460 nm)
- Narrow emission (fwhm < 30 nm)
- High QY (up to 80 %)

Synthesis

- Straightforward (one-pot synthesis)
- Highly reproducible (± 3 nm in PL)
- Scale-up capability (in gram scale)

1st S Injection	Cd _{1-x} Zn _x S (Core)				2nd S Injection	Cd _{1-x} Zn _x S/ZnS (Core/Shell)			
	Cd : Zn	Size	PL λ_{max}	QY (Φ)		Cd : Zn	Size	PL λ_{max}	QY (Φ)
1.2 mmol	0.76 : 0.24	5.4 nm	467 nm	< 5 %	8 mmol	0.14 : 0.86	9 nm	461 nm	42 %
1.5 mmol	0.72 : 0.28	5.1 nm	460 nm	< 5 %	8 mmol	0.15 : 0.85	8.5 nm	450 nm	62 %
1.7 mmol	0.70 : 0.30	5.2 nm	450 nm	< 5 %	8 mmol	0.16 : 0.84	8.7 nm	443 nm	70 %
2.0 mmol	0.58 : 0.42	4.7	441 nm	< 5 %	8 mmol	0.16 : 0.84	8.2 nm	433 nm	81 %
2.2 mmol	0.51 : 0.49	4.5 nm	429 nm	< 5 %	8 mmol	0.16 : 0.84	8.5 nm	422 nm	68 %
2.7 mmol	0.49 : 0.51	4.3 nm	423 nm	< 5 %	8 mmol	0.15 : 0.85	7.5 nm	415 nm	48 %

* Reaction conditions: Cd 1 mmol, Zn 10 mmol, OA 7 ml, ODE 15 ml, T_{injection} 300 °C and T_{growth} 310 °C